

# Isotopic Tracing of Nutrient Sources and Inputs to North-Central Florida Bay

Joshua Linenfelser (✉ [jline006@fiu.edu](mailto:jline006@fiu.edu))

Florida International University College of Arts Sciences & Education <https://orcid.org/0009-0001-7169-5271>

**William Ryan James**

Florida International University College of Arts Sciences & Education

**Ryan J Rezek**

Coastal Carolina University

**Rolando O. Santos**

Florida International University College of Arts Sciences & Education

**Tom A Frankovich**

Florida International University College of Arts Sciences & Education

**Christopher J Madden**

South Florida Water Management District

**James A Nelson**

University of Louisiana at Lafayette

**Jennifer Rehage**

Florida International University College of Arts Sciences & Education

---

## Research Article

**Keywords:** nutrients, nitrogen, stable isotopes, estuary, Florida Bay, algae

**Posted Date:** August 16th, 2023

**DOI:** <https://doi.org/10.21203/rs.3.rs-3228073/v1>

**License:**  This work is licensed under a Creative Commons Attribution 4.0 International License.

[Read Full License](#)

---

1 **Title:** Isotopic Tracing of Nutrient Sources and Inputs to North-Central Florida Bay

2 **Author names:** Joshua O. Linenfelser, [jline006@fiu.edu](mailto:jline006@fiu.edu), Florida International University (Departement of Earth

3 and Environment), Miami (FL), USA, ORCID ID: 0009-0001-7169-5271; W. Ryan James, [wjames@fiu.edu](mailto:wjames@fiu.edu),

4 Florida International University (Department of Earth and Environment), Miami (FL), USA; Ryan J. Rezek,

5 [rrezek@coastal.edu](mailto:rrezek@coastal.edu), Coastal Carolina University, South Carolina, USA, ORCID ID: 0000-0002-3054-6384;

6 Rolando O. Santos, [rsantosc@fiu.edu](mailto:rsantosc@fiu.edu), Florida International University (Department of Biological Sciences), Miami

7 (FL), USA, ORCID ID: 0000-0002-3885-9406; Tom A. Frankovich, [tfrankov@fiu.edu](mailto:tfrankov@fiu.edu), Florida International

8 University, Miami (FL), USA; Christopher J. Madden, [cmadden@sfwmd.gov](mailto:cmadden@sfwmd.gov), South Florida Water Management

9 District, Miami (FL), USA; James A. Nelson, [james.nelson@louisiana.edu](mailto:james.nelson@louisiana.edu), University of Louisiana at Lafayette,

10 Louisiana, USA, ORCID ID: 0000-0003-4607-3953; Jennifer S. Rehage, [rehagej@fiu.edu](mailto:rehagej@fiu.edu), Florida International

11 University, Miami (FL), USA, ORCID ID: 0000-0003-0009-6906

## 12 **Acknowledgment**

13 We thank our collaborators at the South Florida Water Management District (SFWMD), Everglades National Park,

14 Florida International University, the Florida Coastal Everglades Long-term Ecological Research program (FCE

15 LTER), and the CREST Center for Aquatic Chemistry and Environment for their support of our research. We thank

16 Lauren Padron for her assistance with sample preparation, Andy Distrubell and Shakira Trabelsi for their help with

17 field collections, and Mark Kershaw and Marshall Otter for their help with stable isotope analysis. This study was

18 funded by the SFWMD and developed in collaboration with FCE LTER under grants DEB-1832229 and DEB-

19 2025954. The authors have no conflict of interest to declare. This is contribution XX from the Coastlines and

20 Oceans Division of the Institute of Environment at Florida International University.

21

22 **Abstract:** Coastal nutrient loading is a primary driver of changes to habitat structure, species diversity, and  
23 increases in hypoxia and harmful algal blooms in estuaries worldwide. The difficulty of identifying non-point source  
24 inputs of nutrients often hinders the management and mitigation of these nutrient loads. Using stable isotopes, this  
25 study aimed to determine the primary sources of nutrients influencing the coastal Everglades, specifically lake  
26 systems in the rim of north-central Florida Bay. Carbon, nitrogen, and sulfur stable isotope values of algae grown *in*  
27 *situ* were used as a natural tracer of nutrient sources across hydrologic seasons (wet and dry seasons of 2021-2022),  
28 and across a north to south estuarine gradient in these coastal lake systems. Mean  $\delta^{15}\text{N}$  values (+2 to +3‰),  
29 consistent across both space and time, provided evidence that allochthonous N may primarily influence this region.  
30 Mixing models identified a mixture of upstream marsh and downstream bay derived nutrients primarily influencing  
31 the nutrient regime of the systems. Nutrient inputs varied with season and location. We observed higher marsh  
32 derived nutrient inputs in the upper portion of the system during the wet season, and greater nutrient inputs from  
33 Florida bay during the dry season, primarily in the lower portion of the estuary. This study highlights how managed  
34 restoration in marsh waterflow may increase N inputs, however, ecosystem-wide shifts must be better understood to  
35 predict ecological changes.

36 **Key Words:** nutrients, nitrogen, stable isotopes, estuary, Florida Bay, algae

37

## 38 **Introduction**

39 Excess nutrient loading leading to eutrophy and poor water quality are a widespread concern facing coastal  
40 regions worldwide (Nixon et al., 1986; Valiela, 2006; Todd et al., 2019; Malone & Newton, 2020). Globally,  
41 estuarine and coastal waters have shifted from balanced and productive ecosystems to ones experiencing sudden  
42 trophic changes, biogeochemical alterations, and deteriorating habitat quality that can be difficult to revert and thus  
43 can persist for decades, despite restoration efforts (Pinckney et al., 2001; McCrackin et al., 2017). In the United  
44 States and European Union, eutrophic conditions occur in more than half of coastal waters (Breitburg et al., 2018;  
45 Malone & Newton, 2020). Global impacts of coastal nutrient pollution include changes to habitat structure,  
46 decreased biodiversity, and increased hypoxic events and harmful algal blooms (Cloern, 2001; Glibert et al. 2005a,  
47 2005b; Melesse et al., 2008).

48 Sources of nutrients entering estuarine ecosystems can vary, as they are derived from a variety of  
49 anthropogenic and natural processes (Munn et al., 2018; Todd et al., 2019). Estuarine ecosystems are strongly  
50 regulated by hydrologic processes, which control nutrient loading from both marine and terrestrial influences (Koch  
51 et al., 2012). For instance, river runoff and atmospheric deposition contribute to the majority of anthropogenic N in  
52 coastal ecosystems (Howarth et al., 1996; Green et al., 2004; Howarth, 2008; Jickells et al., 2017). Worldwide, over  
53 half of the dissolved inorganic nitrogen (DIN) entering coastal ecosystems is derived from anthropogenic sources  
54 (Galloway et al., 2004; Howarth, 2008; Lee et al., 2016). Natural inputs of nitrogen to coastal systems include  
55 organic matter recycling, riverine inputs, atmospheric deposition, biological N fixation, and onshore transport from  
56 the open ocean (Voss et al., 2011). Globally, 95% of nutrients enter coastal systems through nonpoint (diffuse)  
57 source inputs (Malone & Newton, 2020) and identifying their origin can be a challenge.

58 Stable isotopes have proven to be a powerful tool to identify nutrient sources. Several studies have shown  
59 Nitrogen (N), Carbon (C), and Sulfur (S) stable isotopes to act as useful tracers of nutrients entering coastal  
60 estuarine systems (Kendall et al., 2008; Bruland & Mackenzie, 2010; Swart et al., 2013; Jones et al., 2018; Murphy  
61 et al., 2022). For instance,  $\delta^{15}\text{N}$  ( $^{15}\text{N}/^{14}\text{N}$  isotopic ratio) values have been used to distinguish between  
62 anthropogenically-derived and natural N sources (McClelland & Valiela, 1997; Costanzo et al., 1988; Bannon et al.,  
63 2008; Bruland & Mackenzie, 2010; Swart et al., 2013). Variation in  $\delta^{13}\text{C}$  ( $^{13}\text{C}/^{12}\text{C}$  isotopic ratio) values can be used  
64 to determine rates of production, indicating nutrient availability and temperature (Fry & Wainwright, 1991; Swart et

65 al., 2013). Furthermore,  $\delta^{13}\text{C}$  ratios often produce strong spatial gradients in estuaries, with more enriched  $\delta^{13}\text{C}$  in  
66 marine areas and more depleted values in freshwater reaches, where greater respiration depletes  $\delta^{13}\text{C}$  (O'Leary,  
67 1988; Mook and Tan, 1991; Chanton and Lewis, 1999; Hellings et al., 1999). Differences in  $\delta^{34}\text{S}$  ( $\delta^{34}\text{S}/\delta^{32}\text{S}$  isotopic  
68 ratio) values can distinguish among sources of S derived from porewater vs. rainwater sulfates, sedimentary sulfides,  
69 and S present in the water column, with a gradient of higher enrichment from fresh to marine waters (Fry et al.,  
70 1982; Peterson & Fry, 1987; Connolly et al., 2004).

71 Florida Bay is historically characterized as a highly oligotrophic system containing low surface water N and P  
72 concentrations (Rudnick et al., 1999; Glibert et al., 2009). However, as a product of decades of chronic deficits in  
73 freshwater inflows and resulting hypersalinity, Florida Bay has experienced recurring seagrass die-offs, increased  
74 nutrient concentrations, and persistent algal blooms (Philips & Badylak, 1996; Zieman et al., 1999; Hall et al., 2016;  
75 Glibert et al. 2021). The central region of Florida Bay is where N from Everglades freshwater inputs converges with  
76 P derived from the Gulf of Mexico, making it the region of Florida Bay with the highest chlorophyll-a  
77 concentrations and water column productivity (Fourqurean and Robblee 1999; Madden, 2010). Furthermore, this  
78 region of Florida Bay most prominently displays ecosystem shifts, as it has the lowest freshwater inputs and highest  
79 water residence times, and thus the greatest degree of hydrologic isolation (Glibert et al., 2009; Madden, 2010).  
80 Current efforts to restore the Everglades ecosystem aim to improve the quantity, quality, distribution, and timing of  
81 water flows into Florida Bay (USACE and SFWMD, 2011a; National Academies of Sciences, Engineering, and  
82 Medicine, 2022). Following restoration efforts, studies have shown continued shifts toward greater DIN loading in  
83 the mangrove transition zone at the wetland-bay interface of north-central Florida Bay with subsequent increases in  
84 phytoplankton blooms, primarily consisting of the picocyanobacterium *Synechococcus* spp., that extend out into  
85 central Florida Bay (Shangguan et al., 2017a; Glibert et al., 2021). Although P is the limiting nutrient throughout the  
86 Everglades ecosystem (Rudnick et al., 1999), the *Synechococcus* spp. has numerous physiological mechanisms which  
87 allow for its sustained growth in low phosphate and high ammonium conditions that characterize this region (Glibert  
88 et al. 2021). It is therefore critical that nitrogen sources be identified such that mitigating efforts may be  
89 implemented to reduce and prevent continued excess nitrogen loading.

90 In this study, we used natural abundance stable isotope tracers ( $\delta^{15}\text{N}$ ,  $\delta^{13}\text{C}$ ,  $\delta^{34}\text{S}$ ) to identify the seasonal  
91 sources of nutrients entering the north-central Florida Bay region. We focused primarily on sources of N, and thus

92 used the  $\delta^{15}\text{N}$  isotopic value from algae, collected using *in situ* artificial substrate samplers, as a nitrogen source  
93 tracer. Specifically, our study asked three questions: (1) Is N derived from allochthonous or autochthonous inputs?  
94 (2) What is the mechanism of N input to the system? (3) And how do N-loading mechanisms shift spatially across  
95 water bodies and temporally between hydrologic seasons? Since north-central Florida Bay is relatively distant from  
96 any major anthropogenic influences, we expected little to no anthropogenic nutrient influence and potential sources  
97 of N loads to include atmospheric deposition, surface and groundwater flows,  $\text{N}_2$  biological fixation, internal  
98 recycling processes, and legacy nutrients from historic wading bird rookeries and waterfowl populations (Corbett et  
99 al., 1999; Sutula et al., 2001; Inglett et al., 2011; Owens et al., 2021). We hypothesized that allochthonous inputs  
100 would dominate during the wet season as greater upstream freshwater flow has the potential to transport new N to  
101 the system, while the dry season would primarily be influenced by autochthonous, old nutrients derived from greater  
102 internal recycling processes (Owens et al., 2021; Glibert et al., 2021; Shangguan et al. 2017). We expected spatial  
103 and temporal gradients to follow a trend such that northern areas would experience greater influence from  
104 freshwater marsh-derived nutrients, primarily in the wet season, while the southern portions of the system would be  
105 more influenced by Florida Bay derived nutrient sources, primarily in the dry season (Sutula et al., 2001; Frankovich  
106 et al., 2011).

## 107 **2. Materials and Methods**

### 108 *2.1 Study system*

109 We focused our examination of nutrient sources in two subestuaries at the northern rim of north-central Florida  
110 Bay: the Alligator Creek subestuary (hereafter Alligator) and the McCormick Creek subestuary (hereafter  
111 McCormick), referred to together as the Everglades Coastal Lake Systems (ECLS, Fig. 1). These two lake chains act  
112 as buffers between the Taylor slough drainage and Florida Bay and are considered a main transport vector of  
113 nutrients and chlorophyll *a* to Florida Bay (Shangguan et al., 2017; Glibert et al., 2021). The Alligator lake chain  
114 consists of West Lake, Cuthbert Lake, Long Lake, and the Lungs which leads through Alligator creek into Garfield  
115 Bight, while McCormick contains Seven Palm, Middle Lake, and Monroe Lake, which leads through McCormick  
116 creek into Terrapin Bay (Fig. 1). The northern lakes in each system receive greater freshwater inputs, derived from  
117 both Taylor Slough ground and surface water, while the southern waterbodies are more marine-dominated due to  
118 proximity to Florida Bay (Frankovich et al., 2011; Frankovich et al. 2012; Price et al., 2021). The greatest

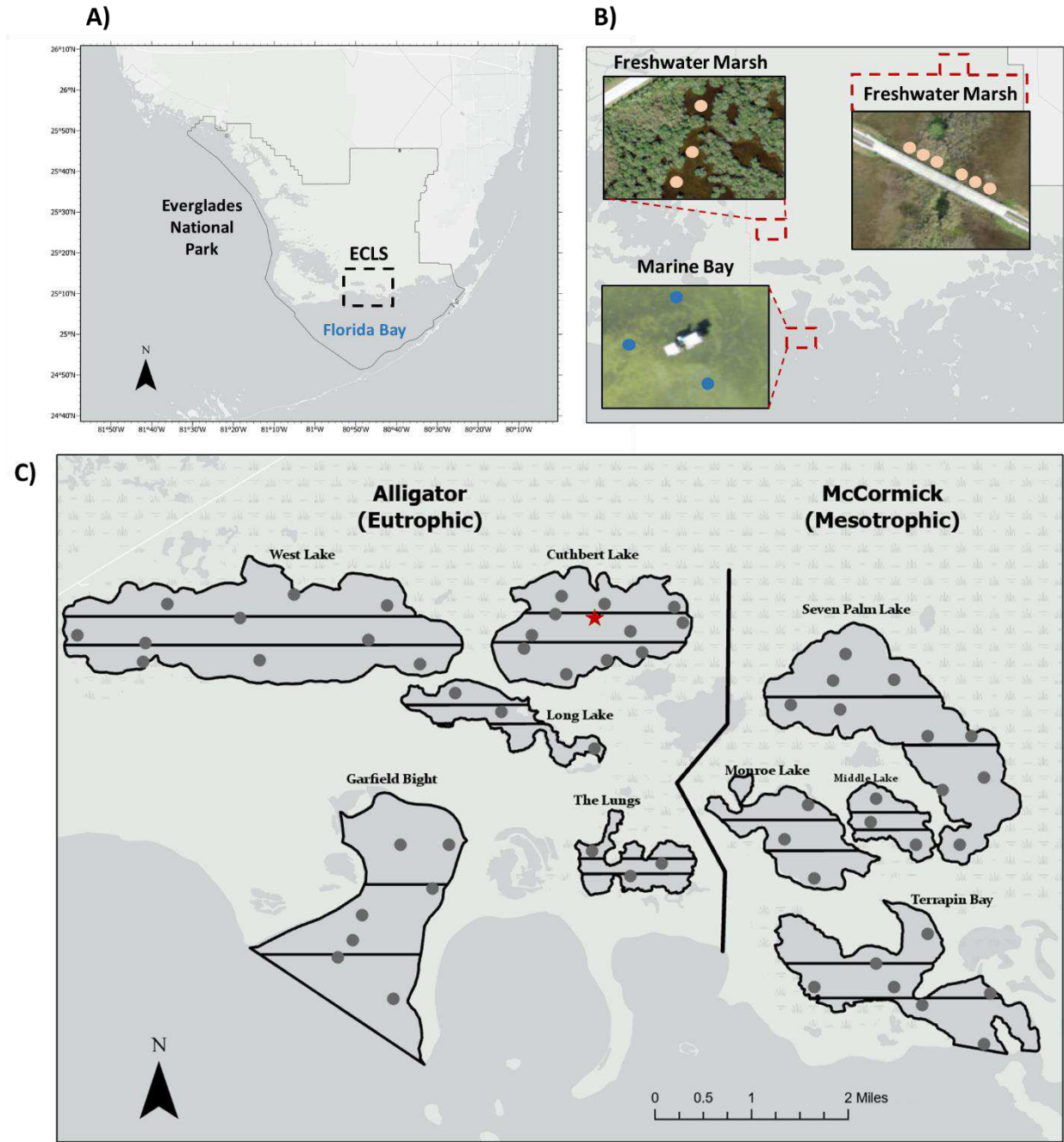


**Fig. 1** A) Location of the Everglades Coastal Lake Systems (ECLS) at the northern rim of north central Florida Bay, Everglades National Park. B) Locations of sampling sites for the freshwater marsh and Florida Bay endmembers used in mixing models. C) Map of all sampling sites in the Alligator and McCormick lake systems. Horizontal lines show strata used for randomization of sites. Red star shows location of the Cuthbert Rookery.

120 contribution of water to both systems is direct precipitation, particularly in the wet season (June-October), with peak  
121 values exceeding 0.3 m/month of rainfall, followed by groundwater, and surface water inputs (Price et al., 2021).  
122 Groundwater discharge is highest in McCormick (2.25 m/yr) compared to only 0.65 m/yr in Alligator (Price et al.,  
123 2021). Both systems exhibit positive groundwater input throughout all months except April in McCormick and  
124 April-May in Alligator (peak of the dry season, Price et al., 2021), when instead, there is a net recharge of  
125 groundwater from the lakes. The semi-enclosed nature of the lake systems makes them susceptible to eutrophic  
126 conditions as they have limited flushing capabilities, allowing for the buildup of nutrients, particularly in Alligator  
127 (Frankovich et al., 2011; Frankovich et al., 2012).

128 The limited freshwater inflow and structural connectivity of Alligator results in seasonally high salinity levels  
129 (>50 ppt) and high-water residence times (estimated at ~ 6 months; Price, 2021; Shangguan et al. 2017a).  
130 Additionally, Alligator contains a bird rookery on a mangrove island in the center of Cuthbert Lake (Ogden et al.  
131 2014, Fig. 1). The rookery was the site of a historical bird megacolony (Ogden et al. 2014), with wading birds  
132 estimated around 6,000 individuals annually (Job, 1905; Chapman, 1908), and today acts as a colony for a much  
133 lower number of wading birds consisting primarily of Wood Storks and Great Egrets that have an annual abundance  
134 of approximately 100 individuals (Cook & Baranski, 2019; Cook & Baranski, 2021). Similar bird rookeries have  
135 been shown to result in increased nutrient concentrations (Wainright et al., 2008). Alligator has trophic state index  
136 values ranging from 54 to 64 characterizing it as a eutrophic system that exhibits high water column nutrient  
137 concentrations, persistent algal blooms, low light availability to the benthos, and less diverse submerged aquatic  
138 vegetation (SAV) cover (Frankovich et al., 2012; Frankovich et al., 2017; Eggenberger et al., 2019). In contrast,  
139 McCormick is closer to the flow path of Taylor Slough and is comprised of relatively short, open, channels  
140 connecting the lake chain to Florida Bay. These topographic characteristics make for greater hydrologic connectivity  
141 to both freshwater inflow and Florida Bay. Consequently, McCormick has lower salinity levels, lower water  
142 residence times (4-5 months; Price, 2021; Price, 2022), and trophic state index values ranging from 40 to 44,  
143 classifying it as mesotrophic with lower nutrients, salinities, and phytoplankton concentrations (Frankovich et al.,  
144 2017, Eggenberger et al., 2019).

## 145 *2.2 Seasonal Sampling*

146 Microalgae samples were collected from 71 samplers deployed seasonally across the ECLS (Fig. 1), at two  
147 freshwater endmember sites located in the marsh upstream of the ECLS (n=9 samples), and at a marine endmember  
148 site located just south of Garfield Bight (n=3 samples, Fig. 1B). The respective endmember sites provided isotopic  
149 values indicative of freshwater and marine nutrients. The two marsh sites were located in freshwater marshes at the  
150 Taylor Slough bridge and upstream of Alligator (685 m from West Lake). Within the ECLS, we used a stratified  
151 random sampling design for site selection, which allowed for a fine-scale spatial variation gradient (Fig. 1C). Each  
152 waterbody was delineated into three equally-sized strata, and sites were randomly selected within each stratum (with  
153 a 600 m buffer around each site). The upstream lakes (West, Cuthbert, Seven Palm) and the downstream bays  
154 (Garfield Bight and Terrapin Bay) had a greater number of sites (10-12 sites) to account for both their larger surface  
155 area and for sites of interest, while the middle lakes had fewer sites due to their relatively small size ( $< 2 \text{ km}^2$ ; 3 sites  
156 each, Fig. 1C). A site of interest in Alligator was the Cuthbert Rookery. Samplers were randomly distributed within  
157 a 50 m radius around the rookery (n=3 sites). Bird excrement was also sampled from the Cuthbert Rookery (n=4  
158 replicates). This sampling scheme totaled 79 samples per season.

159 Sampling was conducted in the wet (Sept-Feb) and dry (Mar-Aug) seasons of 2020-2021, at times matching  
160 the maximum and minimum freshwater inflows (Appendix 1). During both seasons, samplers were deployed for 3-  
161 week sampling periods, where algae grew in situ. Wet season sampling took place from late October through early  
162 November 2021. Due to sampling failure stemming from a portion of algal samplers tipping over with high winds,  
163 16 of the 71 sites were redeployed in mid-November to early December, a time frame still within the yearly salinity  
164 minimum (Appendix 1). Dry season sampling took place in the 3-week period of late April into early May 2022. At  
165 all sites, salinity, temperature, and dissolved oxygen (DO) measurements were taken using a YSI probe, while  
166 turbidity was measured with a Secchi disk at both sampler deployment and pickup (Appendix 2).

### 167 *2.2.1 Sample collection*

168 In aquatic environments, artificial substrate sampling is a useful technique for assessing water quality  
169 (Biggs & Kilroy, 2000). Artificial substrate provides equally-sized, equally-handled, and uniformly-aged algal  
170 growth surfaces, removing unwanted substratum and temporal variability associated with naturally collected  
171 samples (Biggs & Kilroy, 2000; Costanzo et al., 2001; Francoeur et al., 2013). In our study, we deployed an  
172 artificial substrate sampler at each of the 71 sampling sites. We constructed algal samplers using 2 plates of

173 plexiglass and a PVC stake (Appendix 3A-B). Samplers were deployed with the top plate at 30 cm from the surface  
174 to ensure a consistent supply of light and free-flowing water across the substrate surface which are the preferred  
175 conditions for algal growth (Biggs & Kilroy, 2001). Following the three-week soak period in both seasons,  
176 microalgae growth was scraped from plexiglass slides upon collection, and stored in a sampling bag on ice. Upon  
177 return to the lab, samples were frozen at -20° C until processed.

178 Bird excrement was hand collected from the Cuthbert rookery in Cuthbert Lake. Excrement was scraped  
179 from mangrove leaves on the rookery, and birds were identified at the time of sampling. This included Cormorants  
180 and White Egrets (n = < 10) in the wet season, and White Egrets (n = ~100), Wood Storks (n = ~50), and  
181 Cormorants (n = ~ 20) in the dry season. Samples were stored in whirl-paks on ice, then frozen at -20° C until  
182 processed.

### 183 *2.3 Laboratory analyses*

184 The samples were defrosted and run through a 100-micron sieve into a 1000 ml beaker using deionized  
185 water to separate any detritus or shell material from microalgae. A subsample of microalgae was then vacuum  
186 filtered through a pre-combusted 47 mm Whatman GF/F filter. The filtered samples were then dried at 55 °C in a  
187 drying oven for 48 h and then scraped before weighing them. Samples were weighed out between 2.0 to 3.0 mg and  
188 placed in 5 x 9 mm silver capsules for  $\delta^{13}\text{C}$  analysis and in 5 x 9 mm tin capsules for  $\delta^{15}\text{N}$  and  $\delta^{34}\text{S}$  analysis.  
189 Samples in silver capsules used for  $\delta^{13}\text{C}$  analysis were decarbonated using 5% hydrochloric acid to remove ambient  
190 calcium carbonate (Chanton & Lewis 1999). Cuthbert rookery samples were carefully scraped to separate excrement  
191 from mangrove leaf and branch material. Samples were then dried at 55 °C for 48 h and ground to a powder using a  
192 ceramic mortar and pestle. Powdered samples were then weighed out between 0.5 to 0.7 mg and placed in 5 x 9 mm  
193 tin cups for  $\delta^{13}\text{C}$  and  $\delta^{15}\text{N}$  analysis.

194  $\delta^{13}\text{C}$  and  $\delta^{15}\text{N}$  isotopic abundances were determined using elemental combustion analysis on a Carlo Erba  
195 1108 coupled to a DeltaV Plus isotope ratio mass spectrometer via a ConFlo IV interface at Florida International  
196 University. A total of 150 samples were analyzed for C and N including 118 algal samples from the ECLS, 24 algal  
197 samples from the marsh and bay end members, and 8 bird excrement samples.  $\delta^{34}\text{S}$  was analyzed at the Woods Hole  
198 Marine Biological Stable Isotope Laboratory using a Europa 20-20 continuous-flow isotope ratio mass spectrometer  
199 interfaced with a Europa ANCA-SL elemental analyzer. Due to logistical constraints, only a subset of samples were

200 analyzed for S totaling 70 samples including 58 algal samples from the ECLS and 12 samples from the upland  
201 marsh endmember. The analytical precision based on replicate analyses of isotopically homogeneous international  
202 standards is +/- 0.3 ‰ for the  $\delta^{34}\text{S}$  measurement. The results are presented in standard delta notation as parts per  
203 thousand (‰), using international standards of atmospheric nitrogen (air, N<sub>2</sub>), Vienna PeeDee Belemnite (V-PDB)  
204 for Carbon, and Vienna-Canyon Diablo Troilite for Sulfur.

## 205 *2.5 Data Analyses*

206 Ordinary kriging was used to interpolate the geographic distribution of the mean  $\delta^{15}\text{N}$ ,  $\delta^{13}\text{C}$ , and  $\delta^{34}\text{S}$  patterns  
207 across both seasons throughout the ECLS for all 118 algal samples collected. The Ordinary kriging method of  
208 interpolation uses a weighted moving average that's informed by a semivariogram output to produce interpolations.  
209 Ordinary kriging estimates unknown cell values across space by using spatial correlation such that cells near each  
210 known point are given more weight than those farther away (Fletcher & Fortin, 2018). Statistical tests were run  
211 using Bayesian mixing models in R version 4.2.1 (R Core Team, 2021) using the package MixSIAR (v3.1.1, Stock  
212 et al., 2018) to determine the relative resource contributions to algal samples at each site sampled throughout the  
213 ECLS. Models were run for each season with  $\delta^{15}\text{N}$  and  $\delta^{13}\text{C}$  values of algae from each site set as a fixed factor and  
214 the source values derived from the mean  $\delta^{15}\text{N}$  and  $\delta^{13}\text{C}$  of the marsh and bay endmembers combined between  
215 seasons. Ordinary kriging interpolations were used to present the mean proportion of contributions to each site  
216 across the ECLS.

## 217 **3. Results**

### 218 *3.1 Environmental Conditions*

219 Environmental conditions during sampling varied seasonally and across the ECLS, with salinity and  
220 dissolved oxygen showing the highest variation (Appendix 2). Salinity in Alligator (dry = 21.80‰ and wet =  
221 15.94‰) and McCormick (dry = 26.02‰ and wet = 19.02‰) varied similarly between seasons with higher salinity  
222 in the dry compared to the wet season. As expected, salinity was higher in bays and lowest in upstream lakes. DO  
223 levels varied slightly between seasons, and instead varied strongly across systems (Alligator = 5.73 mg/L and  
224 McCormick = 8.08 mg/L), with the lowest DO observed in the Lungs in the dry season (3.2 mg/L). McCormick had  
225 higher light transparency than Alligator (0.62 m vs. 0.49 m), with the lowest transparency also at the Lungs (30.5

226 m). Temperatures stayed relatively consistent across systems (Alligator = 27.14°C vs. McCormick = 26.77°C), with  
 227 little seasonal variation.

228 *3.2 Bulk Isotopic Composition and Spatiotemporal Variation*

229 Microalgal  $\delta^{15}\text{N}$ ,  $\delta^{13}\text{C}$ , and  $\delta^{34}\text{S}$  values varied across systems and seasons but remained in the expected  
 230 isotopic range for estuarine primary producers (Fry et al., 2006; Bouillon et al., 2011; Peterson et al., 1986). The  
 231 overall mean across all samples was  $-23.28\text{‰}$  for  $\delta^{13}\text{C}$ , and  $3.10\text{‰}$  for  $\delta^{15}\text{N}$  (Table 1). There was greater variation  
 232 in  $\delta^{13}\text{C}$  than  $\delta^{15}\text{N}$ , with  $\delta^{13}\text{C}$  ranging between  $-15.55\text{‰}$  to  $-34.20\text{‰}$  across all microalgae samples, whereas  $\delta^{15}\text{N}$

**Table 1.**  $\delta^{15}\text{N}$ ,  $\delta^{13}\text{C}$ , and  $\delta^{34}\text{S}$  values (means  $\pm$  SD) for all algal samples in both seasons throughout the study system, along with mixing model results using the  $\delta^{15}\text{N}$  and  $\delta^{13}\text{C}$  values to determine the proportion of bay and marsh source nutrient inputs to the ECLS.

Season	Stable Isotope Results			Lake	Mixing Model Results	
	$\delta^{15}\text{N}$	$\delta^{13}\text{C}$	$\delta^{34}\text{S}$		Bay	Marsh
				<b>Taylor Slough Endmember</b>		
Wet	3.32 $\pm$ 0.89	-30.67 $\pm$ 2.09	14.32 $\pm$ 2.81	Marsh		
Dry	4.05 $\pm$ 1.09	-30.49 $\pm$ 2.55	11.50 $\pm$ 4.18	Marsh		
				<b>Alligator</b>		
Wet	2.97 $\pm$ 0.87	-21.86 $\pm$ 1.75	7.00 $\pm$ 7.91	West Lake	0.60 $\pm$ 0.14	0.40 $\pm$ 0.14
Dry	2.16 $\pm$ 1.11	-20.78 $\pm$ 1.93	6.75 $\pm$ 4.34	West Lake	0.73 $\pm$ 0.11	0.27 $\pm$ 0.11
Wet	3.61 $\pm$ 0.65	-24.92 $\pm$ 0.31	6.70 $\pm$ 1.65	Cuthbert Lake	0.37 $\pm$ 0.03	0.63 $\pm$ 0.03
Dry	2.88 $\pm$ 0.63	-24.12 $\pm$ 1.08	13.47 $\pm$ 0.84	Cuthbert Lake	0.49 $\pm$ 0.09	0.51 $\pm$ 0.09
Wet	3.22 $\pm$ 0.92	-24.67 $\pm$ 0.74	3.53 $\pm$ 2.46	Long Lake	0.39 $\pm$ 0.06	0.61 $\pm$ 0.06
Dry	2.45 $\pm$ 0.45	-23.73 $\pm$ 1.08	2.27 $\pm$ 1.53	Long Lake	0.53 $\pm$ 0.09	0.47 $\pm$ 0.09
Wet	2.64 $\pm$ 0.30	-24.67 $\pm$ 0.62	1.17 $\pm$ 0.75	The Lungs	0.40 $\pm$ 0.04	0.60 $\pm$ 0.04
Dry	2.41 $\pm$ 0.12	-22.64 $\pm$ 0.17	0.97 $\pm$ 2.34	The Lungs	0.61 $\pm$ 0.01	0.39 $\pm$ 0.01
Wet	2.98 $\pm$ 0.34	-18.39 $\pm$ 2.33	2.17 $\pm$ 3.26	Garfield Bight	0.78 $\pm$ 0.18	0.22 $\pm$ 0.18
Dry	3.10 $\pm$ 0.50	-16.94 $\pm$ 1.11	0.97 $\pm$ 1.76	Garfield Bight	0.87 $\pm$ 0.07	0.13 $\pm$ 0.07
				<b>Cuthbert Rookery</b>		
Wet	2.69 $\pm$ 0.49	-23.34 $\pm$ 1.15	NA	Microalgae		
Dry	3.22 $\pm$ 0.71	-22.58 $\pm$ 1.24	NA	Microalgae		
Wet	7.36 $\pm$ 0.53	-25.67 $\pm$ 4.37	NA	Bird Excrement		
Dry	6.63 $\pm$ 0.73	-28.12 $\pm$ 3.34	NA	Bird Excrement		
				<b>McCormick</b>		
Wet	3.07 $\pm$ 0.51	-25.19 $\pm$ 0.54	-4.97 $\pm$ 2.68	Seven Palm	0.36 $\pm$ 0.04	0.64 $\pm$ 0.04
Dry	2.62 $\pm$ 0.65	-24.02 $\pm$ 1.17	-2.60 $\pm$ 6.07	Seven Palm	0.51 $\pm$ 0.10	0.49 $\pm$ 0.10
Wet	2.39 $\pm$ 0.27	-24.20 $\pm$ 0.14	-5.67 $\pm$ 4.27	Middle Lake	0.44 $\pm$ 0.01	0.56 $\pm$ 0.01
Dry	2.44 $\pm$ 0.41	-22.54 $\pm$ 0.35	-7.53 $\pm$ 3.17	Middle Lake	0.62 $\pm$ 0.03	0.38 $\pm$ 0.03
Wet	3.40 $\pm$ 0.25	-25.73 $\pm$ 0.72	6.17 $\pm$ 1.47	Monroe Lake	0.32 $\pm$ 0.04	0.68 $\pm$ 0.04
Dry	2.02 $\pm$ 0.29	-21.23 $\pm$ 0.98	-1.03 $\pm$ 2.68	Monroe Lake	0.72 $\pm$ 0.06	0.28 $\pm$ 0.06
Wet	4.15 $\pm$ 0.82	-21.05 $\pm$ 1.86	-1.13 $\pm$ 5.44	Terrapin Bay	0.66 $\pm$ 0.14	0.34 $\pm$ 0.14
Dry	4.52 $\pm$ 1.07	-18.56 $\pm$ 1.09	-3.97 $\pm$ 5.33	Terrapin Bay	0.86 $\pm$ 0.04	0.14 $\pm$ 0.04
				<b>Florida Bay Endmember</b>		
Wet	2.81 $\pm$ 0.24	-17.26 $\pm$ 0.84	NA	Bay		
Dry	3.05 $\pm$ 0.13	-16.16 $\pm$ 0.10	NA	Bay		

233 values ranged between 0.05‰ and 6.41‰. Mean  $\delta^{34}\text{S}$  values for algae ranged from -10.9‰ to 19.6‰, with the  
 234 overall mean value at 7.27‰. Across systems, isotopic values differed slightly with Alligator being more depleted  
 235 than McCormick in  $\delta^{15}\text{N}$  (+2.90‰ vs. +3.22‰), and more enriched than McCormick in both  $\delta^{13}\text{C}$  (-22.12‰ vs. -  
 236 22.83‰) and  $\delta^{34}\text{S}$  (+4.65‰ vs. -2.60‰). Wading Bird excrement collected as a potential N source ranged in  $\delta^{15}\text{N}$   
 237 values between 6.63‰ to 10.15‰ and in  $\delta^{13}\text{C}$  between -22.06‰ and -31.20‰.

238 Throughout the ECLS, algal  $\delta^{13}\text{C}$  values showed different spatial patterns between the two lake systems but  
 239 were consistently enriched in the dry season (Fig. 2B, Table 1). In Alligator,  $\delta^{13}\text{C}$  values were on average -23.87‰

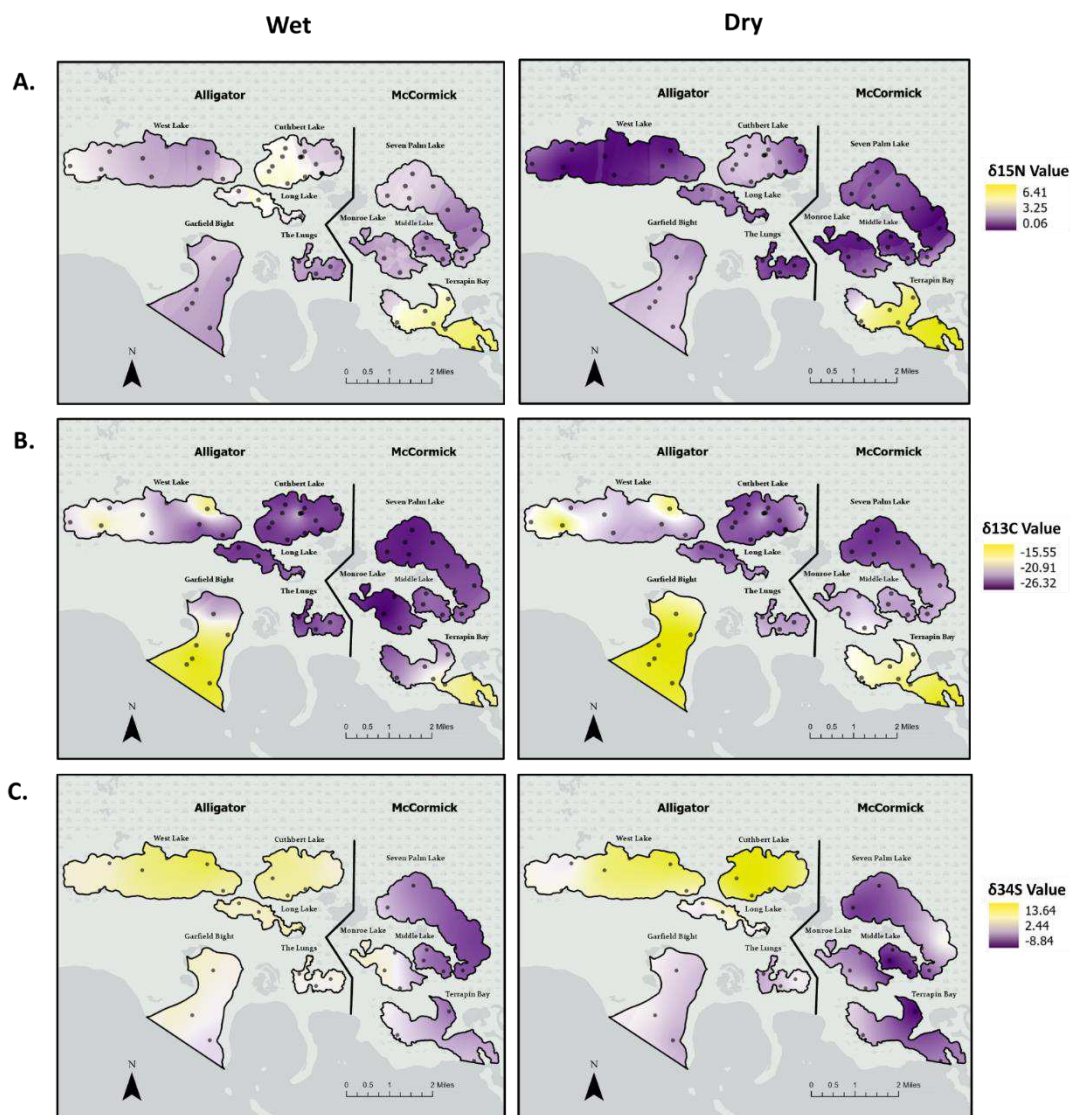


**Fig. 2** Ordinary kriging interpolations showing spatial variation in a)  $\delta^{15}\text{N}$ , b)  $\delta^{13}\text{C}$ , and c)  $\delta^{34}\text{S}$  algal values in the wet and dry seasons across the ECLS. Dots show all sampling sites used in interpolations

240 in the wet and -21.80‰ in the dry season, while in McCormick,  $\delta^{13}\text{C}$  values averaged -22.75‰ in the wet and -  
241 21.51‰ in the dry season. In McCormick, we also saw a strong pattern of increasing  $\delta^{13}\text{C}$  enrichment from the  
242 northern fresher waterbody (Seven Palm) to the southern saltier bay (Terrapin Bay) that was consistent seasonally,  
243 except for Monroe Lake in the wet season having the most depleted values (Fig. 2b). In Alligator, instead of  
244 following a gradient,  $\delta^{13}\text{C}$  values were enriched at the bay site and the uppermost lake (West Lake), with more  
245 depleted values elsewhere (Cuthbert, Long Lake, and The Lungs). Across waterbodies,  $\delta^{13}\text{C}$  was most variable in  
246 West and Monroe Lake and the bay sites, Terrapin Bay and Garfield Bight (Fig. 2b).

247 In contrast to  $\delta^{13}\text{C}$ ,  $\delta^{15}\text{N}$  showed low spatial variability, but a consistent, although less pronounced,  
248 seasonal pattern (Fig. 2a, Table 1).  $\delta^{15}\text{N}$  values were slightly enriched in the wet season in both systems (Alligator  
249 wet = 3.12‰ and dry = 2.68‰; and McCormick wet = 3.35‰ and dry = 3.09‰). Across waterbodies, the most  
250 enriched  $\delta^{15}\text{N}$  values were observed in Terrapin Bay, while the largest seasonal shift was seen in Monroe Lake  
251 (Table 1).  $\delta^{15}\text{N}$  values were the most variable in West Lake and Terrapin Bay, particularly in the dry season (Fig.  
252 2a).

253 For  $\delta^{34}\text{S}$ , we observed contrasting patterns across the lake systems, and inconsistent seasonal differences  
254 (Fig. 2c, Table 1). On average,  $\delta^{34}\text{S}$  values were more enriched in Alligator (wet = 4.29‰ vs. dry = 5.00‰) when  
255 compared to McCormick which displayed more depleted  $\delta^{34}\text{S}$  values (wet = -1.40‰ vs. dry = -3.83‰). The biggest  
256 seasonal shifts were observed in Monroe and Cuthbert lakes and were relatively minor elsewhere. In Alligator, we  
257 observed a marked north-south gradient of enriched to depleted values, while McCormick generally had a more  
258 uniform distribution of relatively depleted values (Fig. 2c).

259 For the freshwater marsh and Florida Bay endmembers,  $\delta^{15}\text{N}$  values were 3.69‰ and 2.93‰ respectively;  
260 which were similar to  $\delta^{15}\text{N}$  values found throughout the ECLS (Table 1). Marsh and bay endmembers  $\delta^{13}\text{C}$  values  
261 were -30.6‰ and -18.7‰ respectively, showing the expected marked variation between marsh and bay-derived C  
262 (Fig. 3). For  $\delta^{34}\text{S}$ , marsh values were enriched, at 12.91‰. And while  $\delta^{34}\text{S}$  at the Florida Bay endmember was not  
263 measured due to logistic constraints, mean  $\delta^{34}\text{S}$  values taken from the combination of Garfield Bight and Terrapin  
264 Bay sites fell at -0.49‰. All three isotopes showed little variation in the endmember sites and were consistent  
265 between seasons.

266 Last, microalgae samples collected in the proximity of the Cuthbert Rookery had mean isotope values of  
 267 +2.69‰ and +3.22‰ for  $\delta^{15}\text{N}$ , and -23.34‰ to -22.57‰ for  $\delta^{13}\text{C}$  in the wet and dry season, respectively (Table 1).  
 268 These values did not differ from those of algae collected elsewhere in Cuthbert Lake (Fig. 2). In contrast, bird  
 269 excrement samples taken from the rookery had more enriched  $\delta^{15}\text{N}$  values (wet = +6.63‰ and dry = +7.36‰), and  
 270 more depleted  $\delta^{13}\text{C}$  values (wet = -28.12‰ and dry = -25.67‰).

271 *3.3 Bulk mixing contributions and spatiotemporal variation*

272 Mixing model results showed that the C and N nutrient load to the ECLS was derived from both marsh and bay  
 273 sources, with a consistently higher contribution of bay nutrients (Table 1). In Alligator, the bay contribution was  
 274 59% relative to 41% marsh contribution, while in McCormick, bay contribution was 56% relative to 44% marsh  
 275 contribution. In both systems, seasonal shifts caused a greater contribution of bay nutrients in the dry season, while  
 276 the wet season had a close to equal mixture of bay and marsh influence. The increased marine contribution in the dry

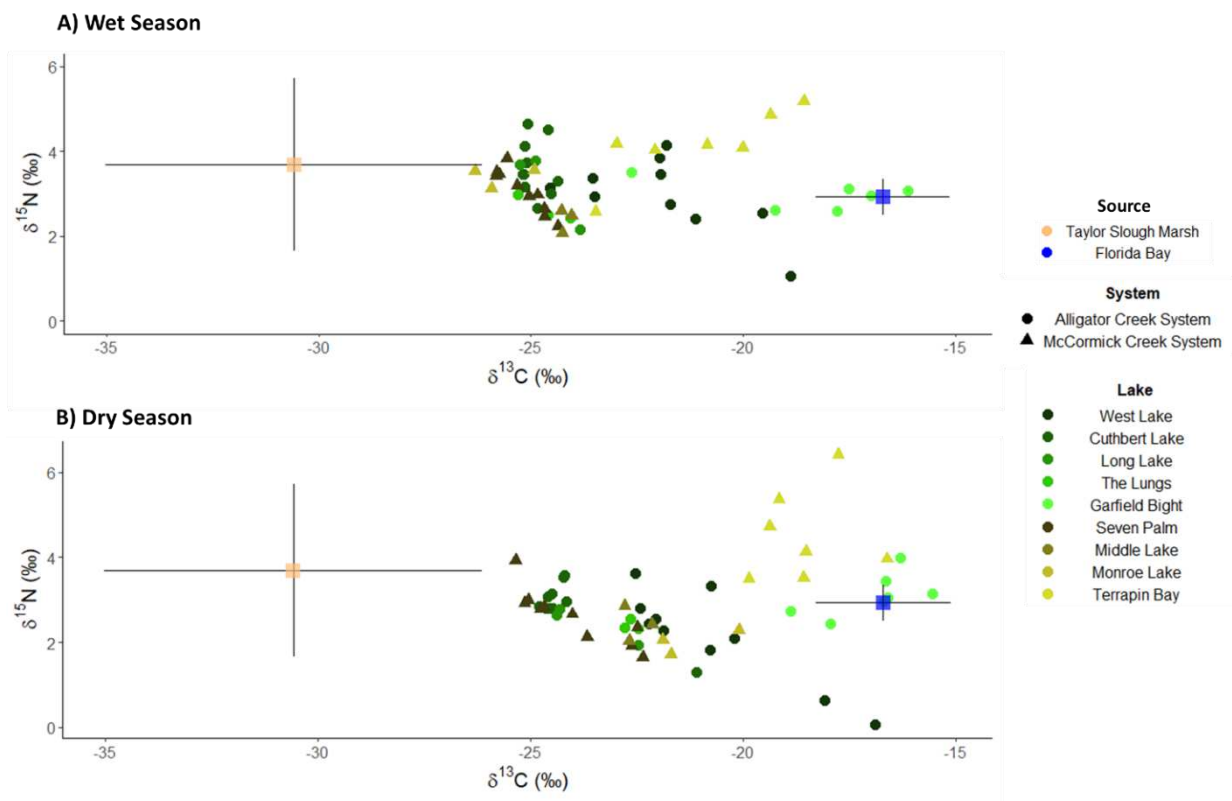


**Fig. 3** Biplots of mean algal  $\delta^{15}\text{N}$  and  $\delta^{13}\text{C}$  values across the a) wet and b) dry seasons for each water body (shades of green are means for the Alligator waterbodies while shades of brown are mean values for the McCormick waterbodies). Shown are also mean (and SD) for the marsh and bay endmembers

277 season resulted in a 66% bay contribution in both Alligator and McCormick, whereas in the wet season, the bay  
278 contribution was lower, at 52% in Alligator vs. 45% in McCormick. Spatially, nutrient contributions followed an  
279 expected trend of greater marsh contribution in the northern lakes to greater bay contribution in the southern  
280 waterbodies (Fig. 3). In Alligator, the greater wet season marsh influence was observed throughout the lakes, except  
281 in West Lake, which had a wet season bay contribution of 60%. In contrast, McCormick showed a pattern of greater  
282 marsh influence in the wet season in Seven Palm, which declined in Middle Lake, and then increased again in  
283 Monroe Lake (Table 1, Fig. 3). In the dry season, McCormick showed equal bay and marsh contributions in Seven  
284 Palm Lake and an increasing pattern of bay influence downstream.

#### 285 **4. Discussion**

286 Globally, coastal and estuarine ecosystems are experiencing increased nutrient loads that hinder ecosystem  
287 health and function (Paerl et al., 2014; Malone & Newton, 2020) The Florida Bay ecosystem faces these same  
288 threats as increasing freshwater flow regimes have been implicated in driving increases in ammonium (NH<sub>4</sub><sup>+</sup>) and  
289 dissolved organic nitrogen (DON) (Shangguan et al., 2017; Glibert et al., 2021). Here, we used  $\delta^{15}\text{N}$ ,  $\delta^{13}\text{C}$ , and  $\delta^{34}\text{S}$   
290 to identify seasonal sources of nitrogen driving production in the Alligator and McCormick systems, located at the  
291 northern rim of Florida Bay. We found that the N load within both systems was primarily allochthonous-derived.  
292 Mixing models showed that C and N loads were derived from both marsh and bay sources, with a greater  
293 contribution of marsh sources in the wet season and greater bay influence in the dry season. As expected, greater  
294 marsh nutrient influence was observed in upstream waterbodies, while greater bay nutrient influence was seen  
295 downstream within these two lake chains.

##### 296 *4.1 Allochthonous vs. Autochthonous Nitrogen*

297 Allochthonous hydrologic inputs that can transport nutrient loads are derived primarily from precipitation, and  
298 surface and groundwater flows from both upstream (freshwater marshes in Taylor Slough) and downstream (Florida  
299 Bay) endmembers. Also, the process of biological N<sub>2</sub> fixation can further contribute to N loading. These sources are  
300 all expected to carry N that is relatively depleted in  $\delta^{15}\text{N}$  (Savoie et al. 1987; McClelland & Valiela, 1997; Bohlke  
301 et al., 2003; Corbett et al., 1999; Rudnick et al., 1999; Price et al., 2021). In contrast, autochthonous N sources such  
302 as legacy nutrients from bird excrement and internal recycling processes have relatively enriched  $\delta^{15}\text{N}$  values  
303 (McClelland & Valiela, 1997). This isotopic variation is the result of fractionation, which occurs as physical,

304 chemical, and biological processes sort isotope species with varying nuclei mass (Sigman & Casciotti, 2001), and  
 305 can be useful for distinguishing between allochthonous and autochthonous nutrient sources. Published  $\delta^{15}\text{N}$  values  
 306 were used to distinguish precipitation, groundwater, and  $\text{N}_2$  fixation as nitrogen sources. Atmospheric deposition  
 307 values range between  $-7\%$  to  $+1\%$ , whereas groundwater discharge values range from  $+2\%$  to  $+8\%$  and  $\text{N}_2$  fixation  
 308 values are close to  $0\%$  (Savoie et al. 1987; Macko & Ostrom, 1994; McClelland & Valiela, 1997; Katz & Bohlke,

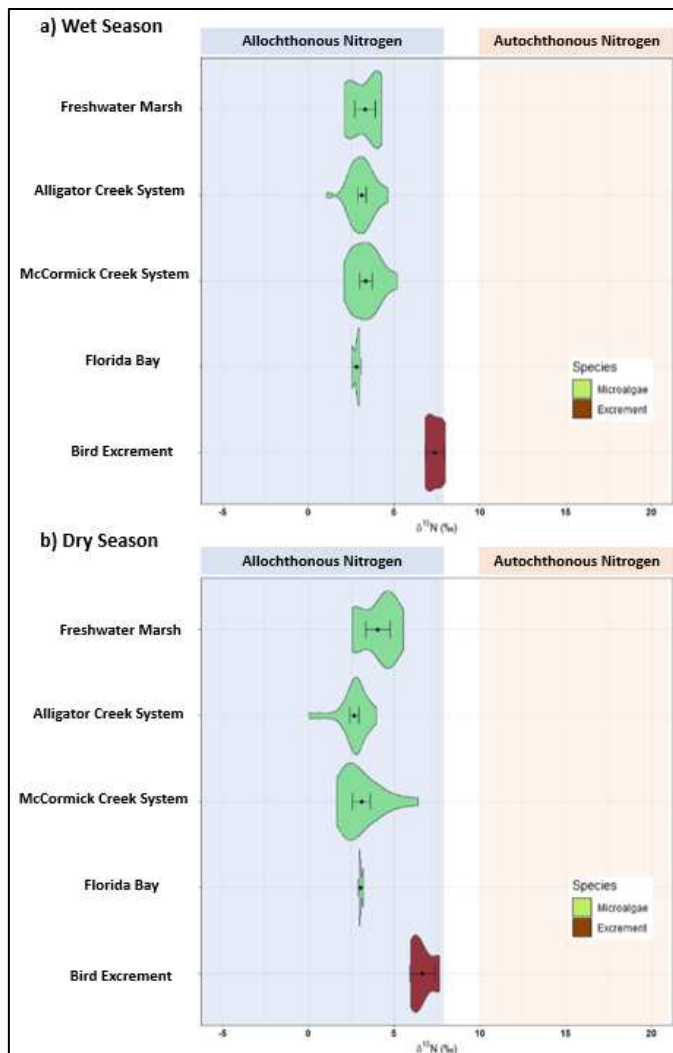


**Fig. 4** Violin plots showing mean (and standard error) algal  $\delta^{15}\text{N}$  values (green) across endmembers (freshwater marsh and Florida Bay), the Alligator and McCormick systems and for bird excrement from the Cuthbert rookery in Alligator (brown) across the a) wet and b) dry seasons. Blue shading indicates the range of  $\delta^{15}\text{N}$  values for allochthonous sources in published studies (Savoie et al. 1987; McClelland & Valiela, 1997; Katz & Bohlke, 2000; Kaatz & Bohlke, 2003; Bruland & Mackenzie, 2010), while orange shading indicates the range of  $\delta^{15}\text{N}$  values for autochthonous sources in published studies (Wainright et al., 1998; McClelland & Valiela, 2001; Sigman & Casciotti, 2001)

309 2000; Bohlke et al., 2003; Bruland & Mackenzie, 2010). Surface water  $\delta^{15}\text{N}$  values were determined from  
 310 assimilated  $\delta^{15}\text{N}$  values taken from our algae samples at the endmember sites, which ranged between  $+3\%$  to  $+4\%$ .

311 Hypothesized autochthonous, old N sources influencing our system included internal recycling processes and  
 312 legacy nutrients from a wading bird rookery. Although there is considerable uncertainty in the isotopic values

313 derived from internal recycling processes, these are expected to fall between +10‰ to +25‰ (Sigman & Casciotti,  
314 2001). N dynamics include long-term internal cycling, nitrification, and denitrification that add and deplete reactive  
315 N leading to an overall enrichment of  $\delta^{15}\text{N}$  values in the residual N pool (Sigman & Casciotti, 2001). Our study  
316 showed average  $\delta^{15}\text{N}$  values of  $\sim 3\%$  throughout the ECLS, suggesting that N recycling has minimal influence in  
317 nutrient loading. The other hypothesized N source, particularly in Alligator, are legacy nutrients derived from  
318 excrement from the Cuthbert rookery, a historic wading bird megacolony (Ogden et al., 2014). Nesting bird colonies  
319 on island rookeries have been shown to produce high nutrient loads, through defecation, which can alter  
320 hydrochemical function in surrounding areas as far as 10 km away (Golovkin & Garkavaya 1975; Staunton Smith &  
321 Johnson 1995; Wainwright et al., 1998; Kolb et al., 2010). Isotopic values of animal waste and bird excrement fall  
322 within a relatively enriched range of +10‰ to +20‰ (Wainwright et al., 1998; McClelland & Valiela, 1998).  
323 Excrement collected at the Cuthbert rookery showed enriched  $\delta^{15}\text{N}$  values of +6.63‰ and +7.36‰, which were  
324 more enriched than the algal values surrounding the rookery (+3.22‰ in the wet and +2.69‰ in the dry season).  
325 This deviation in values points to legacy nutrients not having a major influence on N loads to Alligator.

326        Instead, all of our ECLS algae samples fell within the range of allochthonous sourced N, suggesting that the  
327 primary source of N, in both the wet and dry seasons, is allochthonous derived N (Fig. 4). More specifically, the  
328 majority of samples (94%, 132 out of a total of 141 samples) fell within the isotopic range consistent with N  
329 originating from groundwater discharge and surface water from both freshwater marsh and Florida Bay. The  
330 remaining 9 samples have values between 0‰ and 2‰ which is more consistent with N derived from  $\text{N}_2$  fixation.  
331 This finding agrees with previous work by Owens et al. (2021) in the ECLS, which reported that sediment core  
332 incubations had low benthic nutrient fluxes of soluble reactive phosphorus, nitrate,  $\text{N}_2$ , and ammonium into the  
333 water column, suggesting that nutrient influx is primarily allochthonous, rather than related to internal loading from  
334 a sediment-water nutrient exchange. Allochthonous inputs of nutrients to coastal wetlands occur via biologic and  
335 geologic pathways, however, hydrologic input usually dominates (Likens et al., 2013). We expect that in our system  
336 new nutrients also originate and are transported through hydrologic mechanisms.

#### 337 *4.2 Origin of Nutrients*

338         $\delta^{15}\text{N}$  values in our study indicate that the allochthonous N inputs include surface and/or groundwater flow from  
339 both Florida Bay and freshwater marshes. Studies of marsh hydrology have shown that surface water flow from west

340 of ECLS is negligible (Sutula et al., 2001), leaving surface water inflows primarily driven by managed inputs from  
341 Taylor Slough and the L31W and C-111 canal basins to the east. Rudnick et al. (1999) showed that approximately  
342 90% and 60% of N and P, respectively, are removed from surface water entering Taylor Slough. Thus, we expect  
343 that marsh surface flows primarily contain nutrients derived from the decomposition of autochthonous plant material  
344 in the marsh region closely preceding the ECLS. This is supported by the fact that freshwater entering Florida Bay  
345 tends to be rich in organic material, with high DON and DOC (Glibert et al. 2009; Shangguan et al. 2017a; Wilson  
346 et al., 2018). Furthermore, cyanobacterial mats and red mangroves (*Rhizophora mangle*) in the marsh ecosystem  
347 undergoing N<sub>2</sub> fixation may be an additional source of N transported to the ECLS. Cyanobacterial mats in the  
348 northern Everglades marsh (WCA-2A) were estimated to provide >100 mg N m<sup>-2</sup> d<sup>-1</sup> (Inglett et al., 2004), and red  
349 mangroves have been shown to harbor N<sub>2</sub> fixing diazotrophs which can provide major N inputs to ecosystems  
350 (Woitchik et al., 1997; Reef et al., 2010). N dynamics need to be further investigated to identify the role of N<sub>2</sub> fixers  
351 in this region. Our marsh algal samples were relatively depleted in δ<sup>13</sup>C and δ<sup>15</sup>N and enriched in δ<sup>34</sup>S. This  
352 depletion in δ<sup>13</sup>C is characteristic of an organic-rich environment, where respiration of organic material in the water  
353 column and sediments can cause significant <sup>13</sup>C-depletion of the DIC pool (Chanton and Lewis, 1999). In contrast,  
354 marsh algal δ<sup>34</sup>S values were the most enriched samples collected, indicating the presence of sulfate derived from  
355 diffusion and oxidation of sulfide to sulfate in the sediment and shallow groundwater (Orem et al., 2011).

356 Groundwater flow of nutrients through the karst limestone underlying the Everglades has been shown to  
357 provide as much N and P as surface water to Florida Bay (Fennema et al., 1994; Corbett et al., 1999; Saha et al.,  
358 2011). In the ECLS, groundwater inputs are a greater contributor to water than surface flows (Price et al., 2021). N  
359 and C in groundwater are likely sourced from marsh nutrients, as there is presumably natural organic matter  
360 mineralization seeping through the immediately overlying sub-aqueous carbonate sediments (Shinn et al., 1994;  
361 Bohlke et al., 2003). Similarly, the enriched δ<sup>34</sup>S values in our marsh algal samples are indicative of groundwater-  
362 sourced sulfate. Thus, although we did not collect N, C, and S isotopic samples from groundwater, we can assume  
363 that groundwater would fall into the δ<sup>15</sup>N, δ<sup>13</sup>C, and δ<sup>34</sup>S isotopic range of the overlying marsh. We consider the  
364 upland marsh endmember values in our mixing models to represent both surface and groundwater flow of nutrients  
365 to the ECLS.

366 On the other hand, the Florida Bay endmember has a direct connection with the ECLS at the southern extent of  
 367 both Alligator and McCormick. Here, tidal flow is minimal, such that flow into the lakes from the bay is primarily  
 368 wind-driven (Glibert et al., 2009; Eggenberger et al., 2019), and reverse flow of bay waters upstream has the  
 369 potential to transport nutrient loads into the ECLS. Similar to the marsh endmember, Florida Bay endmember algal  
 370  $\delta^{15}\text{N}$  values were relatively depleted, but bay  $\delta^{13}\text{C}$  values were enriched, possibly indicating DIC sourced from  
 371 decomposing seagrass (typically between -10‰ to -15‰; Fourqurean et al., 2005).  $\delta^{34}\text{S}$  values were not measured at  
 372 the Florida Bay end member, but adjacent sites in Garfield Bight and Terrapin Bay were depleted, which may  
 373 represent  $\delta^{34}\text{S}$  of the bay environment. Depleted  $\delta^{34}\text{S}$  values may be indicative of the assimilation of rainwater  
 374 sulfate (+5‰; Orem et al., 2011) or benthic-pelagic coupling of sedimentary sulfides (~-24‰; Connolly et al.,  
 375 2004).

376 ECLS nutrients could be differentiated as being derived from the freshwater marshes or Florida Bay using  $\delta^{13}\text{C}$   
 377 and  $\delta^{15}\text{N}$  in a two-endmember mixing model. The  $\delta^{34}\text{S}$  values fell outside the range of the mixing model, making it  
 378 an unsuitable tracer of nutrients in our system. Although upstream and downstream sources were not widely  
 379 separated in  $\delta^{15}\text{N}$  isotopic space, they were separated well in  $\delta^{13}\text{C}$  space, allowing for the mixing model to  
 380 differentiate primary nutrient inputs across both space and time. The observed mixing model results followed  
 381 expected trends such that greater freshwater derived nutrients entered the ECLS in the wet season compared to  
 382 marine-derived nutrients that primarily influenced the system in the dry season (Fig. 5). It is important to note,

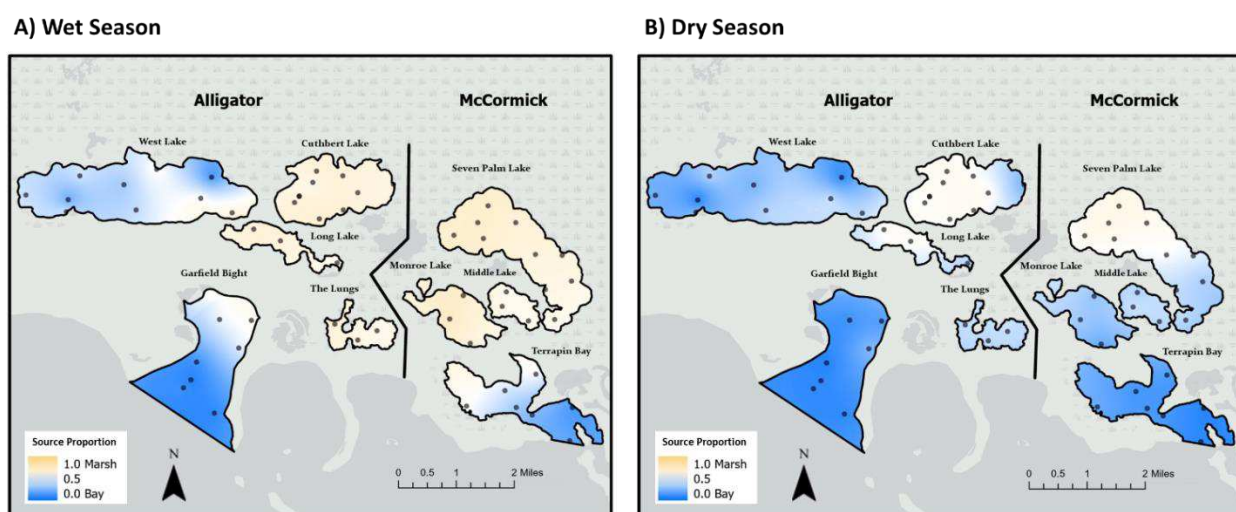


**Fig. 5** Spatial variation in the contribution of bay and marsh nutrients across the ECLS across the a) wet and b) dry seasons. Spatial variation is shown with ordinary kriging interpolations of the mixing model results

383 however, that the results of a mixing model do not account for fractionation effects or for natural variability in  
384 isotopic space at an ecosystem-wide scale, and thus, our mixing model results provide a general understanding of  
385 major nutrient loading mechanisms rather than definitive accounting of all potential sources (Bedard-Haughn et al.  
386 2003; Kendall et al., 2008).

#### 387 4.3 Seasonal shifts and spatial gradients

388 Isotope values in our study portrayed a slightly changing nutrient regime across seasons. Systemwide  $\delta^{15}\text{N}$   
389 values followed a trend of more depleted values in the dry season and enriched values in the wet season. We  
390 hypothesized lower flows in the dry season and subsequent lower flushing of nutrients, which would lead to higher  
391 recycling of nutrients and enrichment of  $\delta^{15}\text{N}$  values. Instead,  $\delta^{15}\text{N}$  values were depleted, which may be a result of  
392 seasonal shifts in nutrient availability. Unpublished data recorded from 2006-2018 from the ECLS showed higher  
393 TN concentrations in the dry season in Alligator (dry = 166.93  $\mu\text{M}$  and wet = 132.83  $\mu\text{M}$ ) and in McCormick (dry =  
394 80.24  $\mu\text{M}$  and wet = 73.0  $\mu\text{M}$ ) (Frankovich, unpubl. data). The availability of N in the surrounding DIN pool can  
395 have a considerable influence on the fractionation of N assimilated in a producer, such as algae, affecting the overall  
396 interpretation of  $\delta^{15}\text{N}$  measurements (Fourqurean et al., 2005). Greater N availability in the dry season allows for  
397 increased fractionation to occur, where algae preferentially assimilate  $^{14}\text{N}$  over  $^{15}\text{N}$  and inherently exhibit more  
398 depleted  $\delta^{15}\text{N}$  values. Fourqurean et al. (2005) recorded a similar seasonal pattern of isotopically light values in  
399 turtle grass (*Thalassia testudinum*) in winter, when reduced plant growth requires lower N and there are higher  
400 concentrations of N available to producers. Seasonal variation in N concentrations may also result from shifts in  
401 submerged aquatic vegetation coverage. The dominant submerged aquatic vegetation in the ECLS is *Chara*  
402 *hornemannii*, whose abundance is strongly regulated by seasonal changes in salinity (particularly those above 25  
403 psu; Frankovich et al., 2011; 2012). Dry season increases in salinity drive seasonal *Chara* die-off events that lead to  
404 elevated  $\text{NH}_4^+$  effluxes and phytoplankton blooms (Owens et al., 2021). Decomposition of *Chara* and phytoplankton  
405 through microbial degradation causes  $\delta^{15}\text{N}$  enrichment in the residual POM, and  $\delta^{15}\text{N}$  depletion in the surrounding  
406  $\text{NH}_4^+$  pool (Liu et al., 1996). Most phytoplankton preferentially uptake  $\text{NH}_4^+$  (Montoya et al., 1991; Velinsky &  
407 Fogel, 1999; Maguer et al., 2000), so it is possible that our samples show slightly depleted  $\delta^{15}\text{N}$  values due to the  
408 assimilation of relatively depleted remineralized  $\text{NH}_4^+$ . In contrast,  $\delta^{13}\text{C}$  values showed a trend of enrichment in the  
409 dry season relative to the wet, likely driven by greater marine-derived carbon entering the ECLS from Florida Bay.

410 In contrast to the seasonality of  $\delta^{13}\text{C}$  and  $\delta^{15}\text{N}$ , algal  $\delta^{34}\text{S}$  did not vary between wet and dry seasons. Instead,  
411  $\delta^{34}\text{S}$  showed marked spatial variation. Although  $\delta^{34}\text{S}$  has the capability to differentiate sources of water entering a  
412 system of interest (Connolly et al., 2004), it may prove an ineffective marker due to the greater influence of marine-  
413 sourced sulfate relative to freshwater sulfates in estuarine habitats (Fry et al., 2002). Pelagic microalgae favors the  
414 assimilation of seawater sulfate due to its greater availability at higher concentrations (generally  $\sim 28$  mM; Fry et al.,  
415 2002), rather than the uptake of freshwater sulfate (often  $< 0.2$  mM; Fry et al., 2002) in all but the lowest salinity  
416 estuarine waters ( $< 1$  PSU; Fry et al., 2002).  $\delta^{34}\text{S}$  values have been shown to remain uniform across estuaries with  
417 open connection to marine waters, making it an unsuitable tracer of water entering these estuaries (Fry et al., 2002).  
418 McCormick has relatively open, short channels connecting the lakes with Florida Bay (Frankovich et al., 2012;  
419 Eggenberger et al., 2019), and our results suggest that McCormick is functioning in this manner, with a uniform  
420 isotopic signal that is relatively depleted in  $\delta^{34}\text{S}$ , similar to values in the downstream bay. Ultimately, although  
421 McCormick receives greater freshwater from Taylor Slough compared to Alligator, it also has a greater connection  
422 to Florida Bay, presumably allowing for higher concentrations of seawater sulfate, which masks the ability of  $\delta^{34}\text{S}$  to  
423 act as a tracer. In contrast, Alligator shows a gradient of more enriched  $\delta^{34}\text{S}$  in upstream lakes to more depleted  
424 values downstream which may be a result of the long, slender creeks which can inhibit the mixing of water masses  
425 (Frankovich et al. 2011). The configuration of Alligator potentially allows for the separation of seawater and  
426 freshwater-derived sulfate across space, allowing producers to uptake and differentiate fresh vs. marine-derived  
427 sulfate.

428 Overall, both systems appear to receive N from the same hydrological mechanisms across both seasons,  
429 receiving greater marsh nutrient contributions in the wet season and greater bay contributions in the dry season (Fig.  
430 6). We expect that the hydrologic characteristics of the lake systems directly regulate nutrient loading mechanisms  
431 across the north-to-south gradient in the lake chains. Both systems show a greater influence of marsh-derived C and  
432 N in the northern water bodies, while the southern waterbodies are more influenced by Florida Bay nutrients. This  
433 finding agrees with Price (2022), where surface waters in both McCormick and Alligator are described as a mixture  
434 of upland marsh and Florida Bay waters, further implicating hydrologic processes as nutrient transport mechanisms  
435 to the ECLS. Yet, West Lake and Monroe Lake deviate from these gradients. West Lake exhibits greater bay  
436 influence than expected given its upstream placement. An ECLS water budget (Price, 2021) describes West Lake as  
437 having the least surface water and groundwater discharge, with main hydrologic inputs instead stemming from

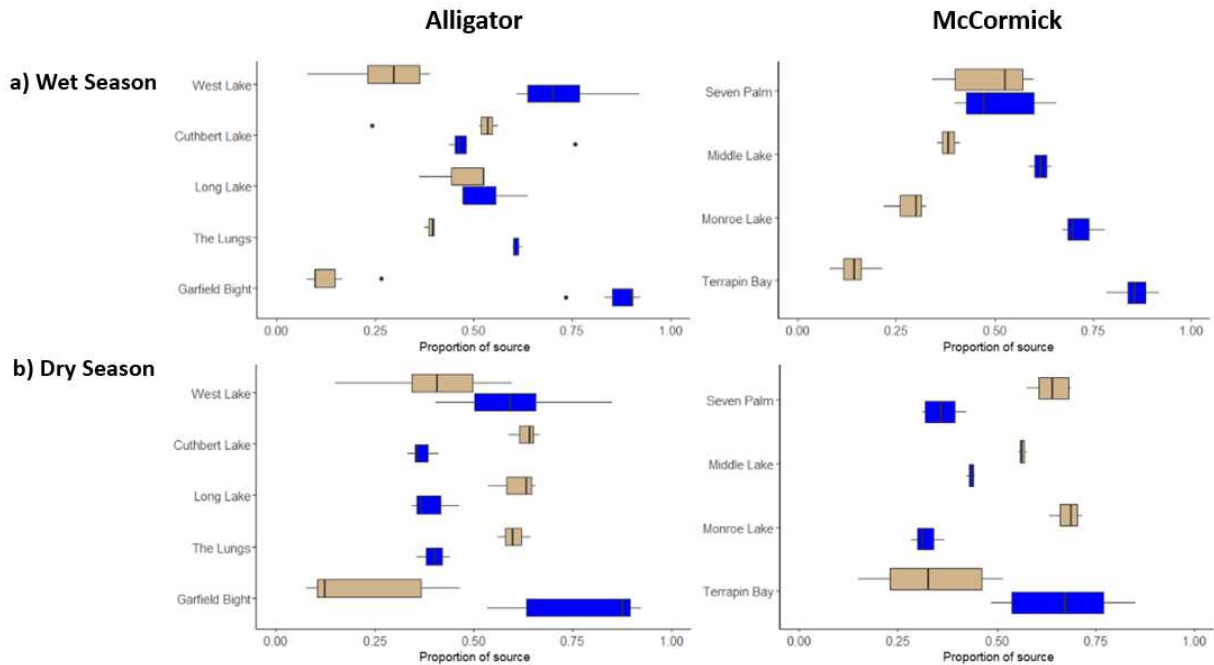


**Fig. 6** Boxplot showing variation in the contribution of marsh and bay sources across waterbodies in Alligator and McCormick across the a) wet and b) dry seasons

438 rainwater and Florida Bay surface water. These findings point to the possibility that an influx of bay nutrients into  
 439 West Lake during the dry season is not flushed out by wet season freshwater influence due to its limited  
 440 connectivity. Monroe Lake also stood out as an exception, showing a wet season increase in marsh nutrients despite  
 441 its downstream placement. This matches water budget data where Monroe Lake has an unknown water source,  
 442 suspected to be the result of either an influx of groundwater discharge or overland flow (Price, 2021).

### 443 5. Summary and implications

444 Ongoing hydrologic restoration efforts aim to increase freshwater flows to the coastal Everglades and Florida  
 445 Bay (Sklar et al. 2019), and there is a need to understand the role of increased flows on nutrient regimes. The  
 446 objective of this study was to determine the major N sources to the ECLS with the goal of gaining a better  
 447 understanding of how changing freshwater flow dynamics will influence regional nutrient regimes. Our findings  
 448 indicate allochthonous nutrient inputs derived primarily from upstream marsh and downstream bay water sources.  
 449 Upstream freshwater flow transports reactive forms of N that could increase N loading to the ECLS. Nutrient  
 450 enrichment of these waters could increase general productivity of the system and enhance the possibility of  
 451 phytoplankton blooms in north-central Florida Bay. At the same time, increased flows will also result in a variety of

452 ecological changes that may act as a buffer to N loading into Florida Bay. For instance, increased freshwater flow  
453 has been shown to reduce the maximum dry season salinities (Sklar et al., 2019), promoting SAV diversity and  
454 community stability throughout the ECLS (National Academies of Sciences, Engineering, and Medicine, 2022).  
455 SAV is a keystone community in Florida Bay that provides many important physicochemical functions aiding in  
456 sediment stabilization, nutrient assimilation, and reducing benthic nutrient exchange to the water column (Yarbro  
457 and Carlson 2008; Glibert et al., 2009; Owens et al., 2021). The ability of SAV to sequester nutrients and counteract  
458 nutrient loading impacts with continued restoration initiatives needs further consideration.

459 Estuaries worldwide face challenges from coastal nutrient loading affecting water quality and in turn altering  
460 the flora and fauna of the aquatic community. It is estimated that ~24% of anthropogenic N delivered to coastal  
461 watersheds reach coastal environments (Malone & Newton, 2020). The findings of this study further demonstrate  
462 the usefulness of  $\delta^{15}\text{N}$ ,  $\delta^{13}\text{C}$ , and  $\delta^{34}\text{S}$  as tracers of coastal nutrient loads and transport pathways, providing essential  
463 information necessary for proper mitigation and reduction of nutrient loading to coastal ecosystems.

464

465

466

467

468

469

470

471

472

473

474

475

476 **References**

- 477 Bannon RO, Roman CT. 2008. Using stable isotopes to monitor anthropogenic nitrogen inputs to estuaries. *Ecol*  
478 *Appl* 18:22–30.
- 479 Bedard-Haughn A, van Groenigen JW, van Kessel C. 2003. Tracing <sup>15</sup>N through landscapes: potential uses and  
480 precautions. *J Hydrol* 272:175–90.
- 481 Biggs BJB, Kilroy C. 2000. *Monitoring Manual Stream Periphyton*.
- 482 Böhlke JK, Shinn E, Reich C, Tihansky A. 2003. Origins and isotopic characteristics of dissolved nitrogen species  
483 in ground water, imported domestic water, and wastewater in the Florida Keys. *US Geol Surv Gt*  
484 *Everglades Sci Program 2002 Bienn Rep US Geol Surv Open-File Rep:03–54*.
- 485 Breitburg D, Levin LA, Oschlies A, Grégoire M, Chavez FP. other authors. 2018. Declining oxygen in the global  
486 ocean and coastal waters. *Science* 359.
- 487 Bruland GL, MacKenzie RA. 2010. Nitrogen Source Tracking with  $\delta^{15}\text{N}$  Content of Coastal Wetland Plants in  
488 Hawaii. *J Environ Qual* 39:409–19.
- 489 Chanton JP, Lewis FG. 1999. Plankton and dissolved inorganic carbon isotopic composition in a river-dominated  
490 estuary: Apalachicola Bay, Florida. *Estuaries* 22:575–83.
- 491 Chapman FM. 1908. *Camps and cruises of an ornithologist* (D. Appleton and Co., New York). *ChapmanCamps*  
492 *Cruises Ornithol*.
- 493 Cloern JE. 2001. Our evolving conceptual model of the coastal eutrophication problem. *Mar Ecol Prog Ser* 210:223–  
494 53.
- 495 Connolly RM, Guest MA, Melville AJ, Oakes JM. 2004. Sulfur stable isotopes separate producers in marine food-  
496 web analysis. *Oecologia* 138:161–7.
- 497 Corbett DR, Chanton J, Burnett W, Dillon K, Rutkowski C, Fourqurean JW. 1999. Patterns of groundwater  
498 discharge into Florida Bay. *Limnol Oceanogr* 44:1045–55.

499 Eggenberger CW, Santos RO, Frankovich TA, James WR, Madden CJ, Nelson JA, Rehage JS. 2019. Coupling  
500 telemetry and stable isotope techniques to unravel movement: Snook habitat use across variable nutrient  
501 environments. *Fish Res* 218:35–47.

502 Fennema RJ, Neidrauer CJ, Johnson RA, MacVicar TK, Perkins WA. 1994. A computer model to simulate natural  
503 Everglades hydrology. *Everglades Ecosyst Its Restor*:249–89.

504 Fletcher R, Fortin M-J. 2018. *Spatial Ecology and Conservation Modeling*.

505 Fourqurean JW, Escorcía SP, Anderson WT, Zieman JC. 2005. Spatial and seasonal variability in elemental content,  
506  $\delta^{13}\text{C}$ , and  $\delta^{15}\text{N}$  of *Thalassia testudinum* from South Florida and its implications for ecosystem studies.  
507 *Estuaries* 28:447–61.

508 Fourqurean JW, Robblee MB. 1999. Florida Bay: A history of recent ecological changes. *Estuaries* 22:345–57.

509 Frankovich TA, Barr JG, Morrison D, Fourqurean JW. 2012. Differing temporal patterns of *Chara hornemannii*  
510 cover correlate to alternate regimes of phytoplankton and submerged aquatic-vegetation dominance. *Mar*  
511 *Freshw Res* 63:1005–14.

512 Frankovich TA, Morrison D, Fourqurean JW. 2011. Benthic Macrophyte Distribution and Abundance in Estuarine  
513 Mangrove Lakes and Estuaries: Relationships to Environmental Variables. *Estuaries Coasts* 34:20–31.

514 Frankovich TA, Rudnick DT, Fourqurean JW. 2017. Light attenuation in estuarine mangrove lakes. *Estuar Coast*  
515 *Shelf Sci* 184:191–201.

516 Fry B. 2006. *Stable isotope ecology*. Springer

517 Fry B, Scalán RS, Winters JK, Parker PL. 1982. Sulphur uptake by salt grasses, mangroves, and seagrasses in  
518 anaerobic sediments. *Geochim Cosmochim Acta* 46:1121–4.

519 Fry B, Smith TJ. 2002. Stable isotope studies of red mangroves and filter feeders from the Shark River estuary,  
520 Florida. *Bull Mar Sci* 70:871–90.

521 Fry B, Wainright SC. 1991. Diatom sources of <sup>13</sup>C-rich carbon in marine food webs. *Mar Ecol Prog Ser* 76:149–57.

522 Galloway JN, Dentener FJ, Capone DG, Boyer EW, Howarth RW, Seitzinger SP, Asner GP, Cleveland CC, Green  
523 PA, Holland EA. 2004. Nitrogen cycles: past, present, and future. *Biogeochemistry* 70:153–226.

524 Glibert PM, Heil CA, Madden CJ, Kelly SP. 2021. Dissolved organic nutrients at the interface of fresh and marine  
525 waters: flow regime changes, biogeochemical cascades and picocyanobacterial blooms—the example of  
526 Florida Bay, USA. *Biogeochemistry* 4. <https://doi.org/10.1007/s10533-021-00760-4>

527 Glibert PM, Heil CA, Rudnick DT, Madden CJ, Boyer JN, Kelly SP. 2009. Florida Bay: water quality status and  
528 trends, historic and emerging algal bloom problems. *Contrib Mar Sci* 38:5–17.

529 Glibert PM, Seitzinger S, Heil CA, Burkholder JM, Parrow MW, Codispoti LA, Kelly V. The role of eutrophication  
530 in the global proliferation of harmful algal blooms. *Oceanography*. 2005a:198–209.

531

532 Glibert PM, Trice TM, Michael B, Lane L. 2005b. Urea in the tributaries of the Chesapeake and coastal bays of  
533 Maryland. *Water Air Soil Pollut* 160:229–43.

534 Golovkin AN, Garkavaya GP. 1975. Fertilization of waters off the Murmansk coast by bird excreta near various  
535 types of colonies. *Sov J Mar Biol* 1:345–51.

536 Green PA, Vörösmarty CJ, Meybeck M, Galloway JN, Peterson BJ, Boyer EW. 2004. Pre-industrial and  
537 contemporary fluxes of nitrogen through rivers: a global assessment based on typology. *Biogeochemistry*  
538 68:71–105.

539 Hall MO, Furman BT, Merello M, Durako MJ. 2016. Recurrence of *Thalassia testudinum* seagrass die-off in Florida  
540 Bay, USA: Initial observations. *Mar Ecol Prog Ser* 560:243–9.

541 Howarth RW. 2008. Coastal nitrogen pollution: a review of sources and trends globally and regionally. *Harmful*  
542 *Algae* 8:14–20.

543 Howarth RW, GBillen; DSwaney; ATownsend; A JAWORSKI ET AL. 1996. Regional nitrogen budgets and  
544 riverine N & P fluxes for the drainages to North Atlantic Ocean: Natural and human influences.  
545 *Biogeochemistry* 35:75–139.

546 Inglett PW, Reddy KR, McCormick PV (2004) Periphyton chemistry and nitrogenase activity in a northern  
547 Everglades ecosystem. *Biogeochemistry* 67:213–233.  
548 <https://doi.org/10.1023/B:BIOG.0000015280.44760.9a>

549 Inglett PW, Rivera-Monroy VH, Wozniak JR. 2011. Biogeochemistry of nitrogen across the everglades landscape.  
550 *Crit Rev Environ Sci Technol* 41:187–216.

551 Jickells TD, Buitenhuis E, Altieri K, Baker AR, Capone D, Duce RA, Dentener F, Fennel K, Kanakidou M,  
552 LaRoche J. 2017. A reevaluation of the magnitude and impacts of anthropogenic atmospheric nitrogen  
553 inputs on the ocean. *Glob Biogeochem Cycles* 31:289–305.

554 Job HK. 1905. *Wild wings: adventures of a camera-hunter among the larger wild birds of North America on sea and*  
555 *land.* Houghton, Mifflin

556 Jones BL, Cullen-unsworth LC, Unsworth RKF, Simon J. 2018. Tracking Nitrogen Source Using  $\delta^{15}\text{N}$  Reveals  
557 Human and Agricultural Drivers of Seagrass Degradation across the British Isles. 9:1–10.

558 Katz BG, Böhlke JK. 2000. Monthly variability and possible sources of nitrate in ground water beneath mixed  
559 agricultural land use, Suwannee and Lafayette Counties, Florida. US Geological Survey

560 Kendall C, Elliott EM, Wankel SD. 2008. Tracing Anthropogenic Inputs of Nitrogen to Ecosystems. *Stable Isot Ecol*  
561 *Environ Sci Second Ed*:375–449.

562 Koch GR, Childers DL, Staehr PA, Price RM, Davis SE, Gaiser EE. 2012. Hydrological Conditions Control P  
563 Loading and Aquatic Metabolism in an Oligotrophic, Subtropical Estuary. *Estuaries Coasts* 35:292–307.

564 Kolb GS, Ekholm J, Hambäck PA. 2010. Effects of seabird nesting colonies on algae and aquatic invertebrates in  
565 coastal waters. *Mar Ecol Prog Ser* 417:287–300.

- 566 Lee RY, Seitzinger S, Mayorga E. 2016. Land-based nutrient loading to LMEs: a global watershed perspective on  
567 magnitudes and sources. *Environ Dev* 17:220–9.
- 568 Likens GE. 2013. *Biogeochemistry of a forested ecosystem*. Springer Science & Business Media
- 569 Liu K-K, Su M-J, Hsueh C-R, Gong G-C. 1996. The nitrogen isotopic composition of nitrate in the Kuroshio Water  
570 northeast of Taiwan: Evidence for nitrogen fixation as a source of isotopically light nitrate. *Mar Chem*  
571 54:273–92.
- 572 Macko SA, Ostrom NE. 1994. Sources of variation in the stable isotopic composition of plants, p. 45-62. In K.  
573 Lajtha and R. H. Michener [eds.], *Stable isotopes in ecology*. Blackwell.
- 574
- 575 Madden CJ. 2010. *Nutrients in Estuaries A Summary Report of the National Estuarine Experts Workgroup 2005–*  
576 *2007*. :155–66.
- 577 Maguer J-F, L’helguen S, Le Corre P. 2000. Nitrogen uptake by phytoplankton in a shallow water tidal front. *Estuar*  
578 *Coast Shelf Sci* 51:349–57.
- 579 Malone TC, Newton A. 2020. The globalization of cultural eutrophication in the coastal ocean: causes and  
580 consequences. *Front Mar Sci*:670.
- 581 McClelland JW, Valiela I. 1998. Linking nitrogen in estuarine producers to land-derived sources. *Limnol Oceanogr*  
582 43:577–85.
- 583 McCrackin ML, Jones HP, Jones PC, Moreno-Mateos D. 2017. Recovery of lakes and coastal marine ecosystems  
584 from eutrophication: A global meta-analysis. *Limnol Oceanogr* 62:507–18.
- 585 Melesse AM, Krishnaswamy J, Zhang K. 2008. Modeling coastal eutrophication at Florida Bay using neural  
586 networks. *J Coast Res*:190–6.
- 587 Montoya JP, Korrigan SG, McCarthy JJ. 1991. Rapid, storm-induced changes in the natural abundance of  $^{15}\text{N}$  in a  
588 planktonic ecosystem, Chesapeake Bay, USA. *Geochim Cosmochim Acta* 55:3627–38.

589 Munn MD, Frey JW, Tesoriero AJ, Black RW, Duff JH, Lee KE, Maret TR, Mebane CA, Waite IR, Zelt RB. 2018.  
590 Understanding the influence of nutrients on stream ecosystems in agricultural landscapes.  
591 <https://doi.org/10.3133/cir1437>

592 Murphy TE, Molina JT, Quill DM, Billeter PA, Mattes K, Woodland RJ. 2022. Seagrass Stable Isotope  
593 Composition Provides Seascape-Scale Tracking of Anthropogenic Nitrogen Inputs in a Tropical Marine  
594 Lagoon. *Estuaries Coasts*. <https://doi.org/10.1007/s12237-022-01058-w>

595 National Academies of Sciences, Engineering, and Medicine. 2022. Progress Toward Restoring the Everglades: The  
596 Ninth Biennial Review-2022.  
597

598 Nixon SW, Oviatt CA, Frithsen J, Sullivan B. 1986. Nutrients and the productivity of estuarine and coastal marine  
599 ecosystems. *J Limnol Soc South Afr* 12:43–71.

600 Ogden JC, Baldwin JD, Bass OL, Browder JA, Cook MI, Frederick PC, Frezza PE, Galvez RA, Hodgson AB,  
601 Meyer KD. 2014. Waterbirds as indicators of ecosystem health in the coastal marine habitats of southern  
602 Florida: 1. Selection and justification for a suite of indicator species. *Ecol Indic* 44:148–63.

603 O’Leary MH. 1988. Carbon Isotopes in Photosynthesis. *BioScience* 38:328–36.

604 Orem W, Gilmour C, Axelrad D, Krabbenhoft D, Scheidt D, Kalla P, McCormick P, Gabriel M, Aiken G. 2011.  
605 Sulfur in the South Florida ecosystem: Distribution, sources, biogeochemistry, impacts, and management  
606 for restoration. *Crit Rev Environ Sci Technol* 41:249–88.

607 Owens MS, Kelly SP, Frankovich TA, Rudnick DT, Fourqurean JW, Cornwell JC. 2021. Controls on nutrient  
608 cycling in estuarine mangrove lake sediments. *J Mar Sci Eng* 9.

609 Paerl HW, Hall NS, Peierls BL, Rossignol KL. 2014. Evolving paradigms and challenges in estuarine and coastal  
610 eutrophication dynamics in a culturally and climatically stressed world. *Estuaries Coasts* 37:243–58.

611 Peterson BJ, Fry B. 1987. Stable isotopes in ecosystem studies. *Annu Rev Ecol Syst* Vol 18:293–320.

612 Philips EJ, Badylak S. 1996. Spatial variability in phytoplankton standing crop and composition in a shallow inner-  
613 shelf lagoon, Florida Bay, Florida. *Bull Mar Sci* 58:203–16.

614 Pinckney JL, Paerl HW, Tester P, Richardson TL. 2001. The role of nutrient loading and eutrophication in estuarine  
615 ecology. *Environ Health Perspect* 109:699–706.

616 Price RM. 2021. "Continued Measurement of Eco-Hydrological Conditions and Water Budgets of Mangrove Lakes  
617 Region of Everglades National Park." *Deliverable 3 for South Florida Water Management District*.

618 R Core Team. 2021. R: A Language and Environment for Statistical Computing. R Foundation for Statistical  
619 Computing, Vienna. <https://www.R-project.org/>.

620 Reef R, Feller IC, Lovelock CE (2010) Nutrition of mangroves. *Tree Physiol* 30:1148–1160.  
621 <https://doi.org/10.1093/treephys/tpq048>

622 Rudnick DT, Chen Z, Childers DL, Boyer JN, Fontaine TD. 1999. Phosphorus and nitrogen inputs to Florida Bay:  
623 The importance of the Everglades watershed. *Estuaries* 22:398–416.

624 S. D. COSTANZO \*, M. J. O'DONOHUE , W. C. DENNISON, R. L. Loneragan and M. T. 1988. A New Approach  
625 for Detecting and Mapping Sewage Impacts. *S. Mod Healthc* 18:4.

626 Saha AK, Saha S, Sadle J, Jiang J, Ross MS, Price RM, Sternberg LS, Wendelberger KS. 2011. Sea level rise and  
627 South Florida coastal forests. *Clim Change* 107:81–108.

628 Savoie DL, Prospero JM, Nees RT. 1987. Washout ratios of nitrate, non-sea-salt sulfate and sea-salt on Virginia  
629 Key, Florida and on American Samoa. *Atmospheric Environ* 1967 21:103–12.

630 Shangguan Y, Glibert PM, Alexander J, Madden CJ, Murasko S. 2017. Phytoplankton assemblage response to  
631 changing nutrients in Florida Bay: Results of mesocosm studies. *J Exp Mar Biol Ecol* 494:38–53.

632 Shinn EA, Reese RS, Reich CD. 1994. Fate and pathways of injection-well effluent in the Florida Keys. US  
633 Geological Survey

634 Sigman DM, Casciotti KL. 2001. Nitrogen Isotopes in the Ocean. *Encycl Ocean Sci*:1884–94.

635 Sklar FH, Beerens JM, Brandt LA, Coronado-Molina CA, Davis SM, Frankovich T, Madden C, McLean A, Trexler  
636 JC, Wilcox W. 2019. Back to the future: Rebuilding the Everglades.

637 Staunton SJ, Johnson CR. 1995. Nutrient inputs from seabirds and humans on a populated coral cay. *Mar Ecol Prog*  
638 *Ser* 124:189–200

639 Steven N. Francoeur, Steven T. Rier and SBW. 2013. Methods for Sampling and Analyzing Wetland Algae.

640 Stock BC, Jackson AL, Ward EJ, Parnell AC, Phillips DL, Semmens BX. 2018. Analyzing mixing systems using a  
641 new generation of Bayesian tracer mixing models. *PeerJ* 6:e5096.

642 Sutula M, Day JW, Cable J, Rudnick D. 2001. Hydrological and nutrient budgets of freshwater and estuarine  
643 wetlands of Taylor Slough in Southern Everglades, Florida (U.S.A.). *Biogeochemistry* 56:287–310.

644 Swart PK, Anderson WT, Altabet MA, Drayer C, Bellmund S. 2013. Sources of dissolved inorganic nitrogen in a  
645 coastal lagoon adjacent to a major metropolitan area, Miami Florida (USA). *Appl Geochem* 38:134–46.

646 Todd PA, Heery EC, Loke LHL, Thurstan RH, Kotze DJ, Swan C. 2019. Towards an urban marine ecology:  
647 characterizing the drivers, patterns and processes of marine ecosystems in coastal cities. *Oikos* 128:1215–  
648 42.

649 USACE and SFWMD. 2011a. Central and Southern Florida Project Comprehensive Everglades Restoration Plan: C-  
650 111 Spreader Canal Western Project: Final Integrated Project Implementation Report and Environmental  
651 Impact Statement. January 2011.

652

653 Valiela I. 2009. Global coastal change. John Wiley & Sons

654 Velinsky DJ, Fogel ML. 1999. Cycling of dissolved and particulate nitrogen and carbon in the Framvaren Fjord,  
655 Norway: stable isotopic variations. *Mar Chem* 67:161–80.

656 Voss M, Baker A, Bange HW, Conley D, Deutsch B, Engel A, ... & Slomp, C. 2011. Nitrogen processes in coastal  
657 and marine ecosystems. Cambridge University Press.

658

659 Wainright SC, Haney JC, Kerr C, Golovkin AN, Flint MV. 1998. Utilization of nitrogen derived from seabird guano  
660 by terrestrial and marine plants at St. Paul, Pribilof Islands, Bering Sea, Alaska. *Mar Biol* 131:63–71.

661 Wilson BJ, Servais S, Mazzei V, Kominoski JS, Hu M, Davis SE, Gaiser E, Sklar F, Bauman L, Kelly S. 2018.  
662 Salinity pulses interact with seasonal dry-down to increase ecosystem carbon loss in marshes of the Florida  
663 Everglades. *Ecol Appl* 28:2092–108.

664 Woitchik AF, Ohowa B, Kazungu JM, et al (1997) Nitrogen enrichment during decomposition of mangrove leaf  
665 litter in an east African coastal lagoon (Kenya): Relative importance of biological nitrogen fixation

666 Yarbro LA, Carlson PR. 2008. Community oxygen and nutrient fluxes in seagrass beds of Florida Bay, USA.  
667 *Estuaries Coasts* 31:877–97.

668 Zieman JC, Fourqurean JW. 1999. Seagrass Die-Off in Florida Bay : Long-Term Trends in Abundance and Growth  
669 of Turtle Author ( s): Joseph C . Zieman , James W . Fourqurean and Thomas A . Frankovich Source :  
670 *Estuaries* , Jun ., 1999 , Vol . 22 , No . 2 , Part B : Dedicated Issue : Florida. 22:460–70.

671

## 672 **Statements & Declarations**

### 673 **Funding**

674 This study was funded by the SFWMD and developed in collaboration with FCE LTER under grants DEB-1832229  
675 and DEB-2025954.

### 676 **Competing Interests**

677 The authors have no conflict of interest to declare.

### 678 **Author Contributions**

679 All authors contributed to the study conception and design. Material preparation and data collection were performed  
680 by Joshua Linenfelser. Data analysis was performed by Joshua O. Linenfelser and W. Ryan James. The first draft

681 was written by Joshua O. Linenfelter and all authors provided comments on previous versions of the manuscript. All  
682 authors read and approved the final manuscript.

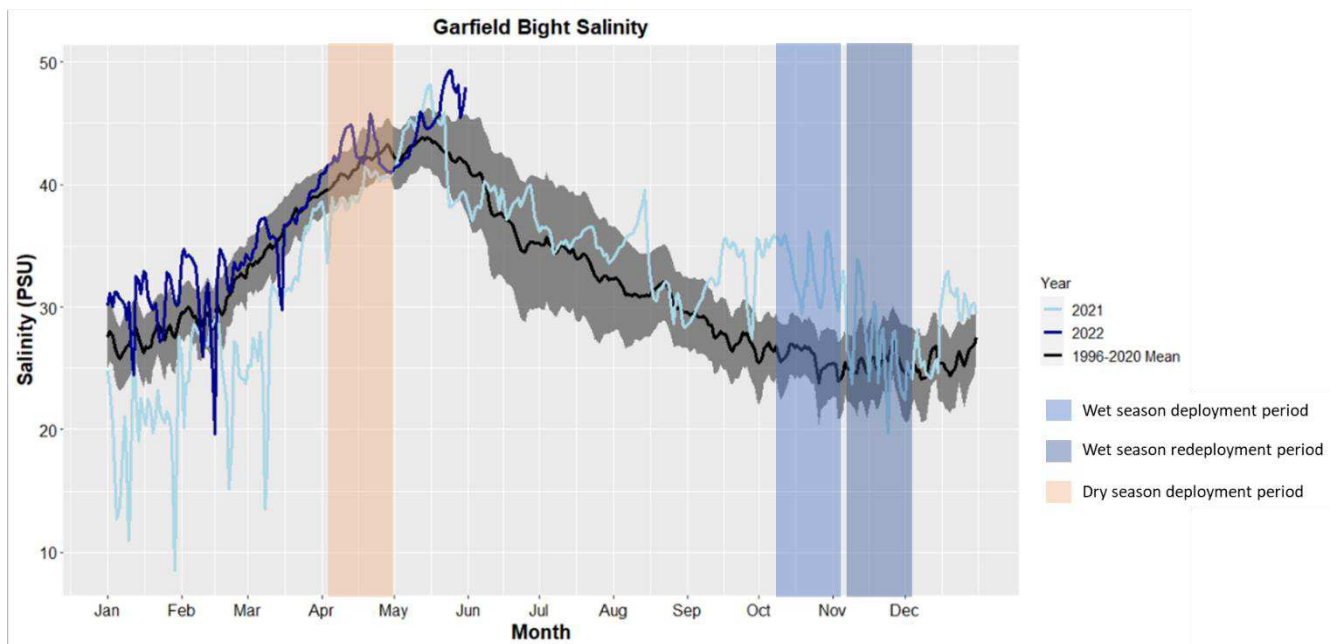
### 683 **Data Availability**

684 Once accepted for publication, all data will be stored in a data repository.

### 685 **Appendices**

686 **Appendix 1.** Salinity conditions at the Garfield Bight hydrological station at the time of sampling in 2021-2022  
687 (blue lines), relative to the 24-year mean (and 95% confidence interval in grey shading). In the ECLS, the wet  
688 season and corresponding minimum salinity lags behind rainfall, such that the lowest salinity is observed in  
689 October-December, while maximum salinity is observed in April-May. Highlighted areas correspond to periods of  
690 algal sampling, which targeted the yearly salinity maximum and minimum.

691



692

693

694

695

696 **Appendix 2.** Environmental conditions (means  $\pm$  SD) across all waterbodies at the time of seasonal sampling.

System & Lakes	Season	Salinity (PSU)	Secchi Depth (m)	Temperature (c)	Dissolved Oxygen (mg/L)
<b>Upland Marsh Endmember</b>					
Marsh	Wet	0.73 $\pm$ 0.95	0.77 $\pm$ 0.23	27.70 $\pm$ 0.60	7.51 $\pm$ 2.60
Marsh	Dry	1.97 $\pm$ 2.61	0.52 $\pm$ 0.14	24.78 $\pm$ 2.78	2.40 $\pm$ 0.88
<b>Alligator</b>					
West Lake	Wet	12.27 $\pm$ 0.47	0.59 $\pm$ 0.10	25.18 $\pm$ 3.40	5.80 $\pm$ 1.30
West Lake	Dry	13.96 $\pm$ 1.04	0.45 $\pm$ 0.07	28.76 $\pm$ 2.04	5.64 $\pm$ 1.94
Cuthbert Lake	Wet	12.10 $\pm$ 0.35	0.52 $\pm$ 0.06	26.27 $\pm$ 2.94	6.72 $\pm$ 1.73
Cuthbert Lake	Dry	13.48 $\pm$ 1.14	0.47 $\pm$ 0.07	29.14 $\pm$ 1.25	6.73 $\pm$ 1.59
Long Lake	Wet	12.42 $\pm$ 0.49	0.45 $\pm$ 0.05	26.37 $\pm$ 3.74	6.63 $\pm$ 0.87
Long Lake	Dry	32.08 $\pm$ 7.46	0.45 $\pm$ 0.05	30.07 $\pm$ 1.26	5.03 $\pm$ 0.96
The Lungs	Wet	17.37 $\pm$ 2.44	0.37 $\pm$ 0.08	26.03 $\pm$ 4.21	6.80 $\pm$ 0.64
The Lungs	Dry	39.17 $\pm$ 13.32	0.33 $\pm$ 0.05	29.78 $\pm$ 1.32	3.19 $\pm$ 1.92
Garfield Bight	Wet	28.70 $\pm$ 3.96	0.48 $\pm$ 0.22	23.90 $\pm$ 3.39	3.67 $\pm$ 1.90
Garfield Bight	Dry	44.84 $\pm$ 1.65	0.52 $\pm$ 0.07	26.71 $\pm$ 3.42	4.17 $\pm$ 1.66
<b>McCormick</b>					
Seven Palm	Wet	13.05 $\pm$ 1.37	0.64 $\pm$ 0.06	25.11 $\pm$ 1.76	7.18 $\pm$ 0.70
Seven Palm	Dry	16.86 $\pm$ 1.76	0.64 $\pm$ 0.09	27.01 $\pm$ 0.62	6.18 $\pm$ 0.49
Middle Lake	Wet	16.03 $\pm$ 1.93	0.52 $\pm$ 0.04	26.12 $\pm$ 1.67	7.16 $\pm$ 1.38
Middle Lake	Dry	23.88 $\pm$ 1.59	0.63 $\pm$ 0.05	28.02 $\pm$ 0.52	6.69 $\pm$ 0.74
Monroe Lake	Wet	20.25 $\pm$ 1.96	0.43 $\pm$ 0.05	26.28 $\pm$ 1.78	7.55 $\pm$ 1.72
Monroe Lake	Dry	30.48 $\pm$ 2.12	0.60 $\pm$ 0.06	28.22 $\pm$ 0.32	6.43 $\pm$ 1.24
Terrapin Bay	Wet	28.29 $\pm$ 4.26	0.71 $\pm$ 0.23	26.35 $\pm$ 2.56	6.90 $\pm$ 0.74
Terrapin Bay	Dry	36.14 $\pm$ 1.13	0.87 $\pm$ 0.23	28.59 $\pm$ 0.61	14.75 $\pm$ 30.94
<b>Florida Bay Endmember</b>					
Bay	Wet	34.30 $\pm$ 2.41	0.95 $\pm$ 0.16	23.28 $\pm$ 2.10	5.08 $\pm$ 0.76
Bay	Dry	43.53 $\pm$ 0.06	0.30 $\pm$ 0.00	24.00 $\pm$ 0.17	5.28 $\pm$ 0.24

697

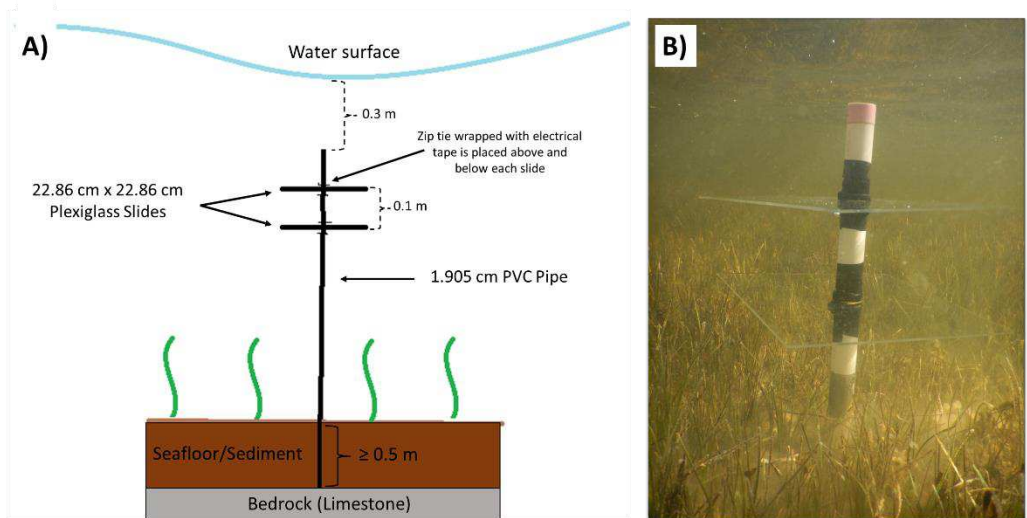
698

699

700

701 **Appendix 3.** Depiction of an algal sampler. A) Each sampler consisted of two 22.86 cm x 22.86 cm clear acrylic  
702 plexiglass zip tied and taped to a 1.9 m PVC pipe staked in the sediment. The plexiglass plates were identical and  
703 were spaced 10 cm apart. The PVC was cut to size such that it could be staked down through the sediment to the  
704 bedrock, at least 0.5 m, and would position the plexiglass to sit exactly 30 cm below the water line. All samplers  
705 were constructed anew for each sampling event. B.) Image of sampler on cement base in area with no sediment.

706



707

708

709

710